https://doi.org/10.5194/egusphere-2026-1514
Preprint. Discussion started: 24 March 2026

Impacts of Shrub Coverage for Arctic Ecosystem Carbon Uptake and Storage

Tamara Emmerichs[1], Fabrice Lacroix[2], Victor Brovkin[1], Sönke Zaehle[3], Cheng Gong[3], Yu Zhu[3,4], Sofie Sjogersten[5], Carolina Voigt[6,7], Klaus Steenberg Larsen[8], and Eeva-Stiina Tuittila[9]

[1]Climate Dynamics, Max Planck Institute for Meteorology, Hamburg, Germany
[2]Institute of Geography, University of Bern, Bern, Switzerland
[3]Department Biogeochemical Signals, Max Planck Institute for Biogeochemistry, Jena, Germany
[4]now at: Institute of Plant Science and Microbiology, University of Hamburg, Hamburg, Germany
[5]Faculty of Science, University of Nottingham, Leicestershire, UK
[6]Permafrost Research Section, Alfred-Wegener Institute Helmholtz Centre for Polar and Marine Research, Potsdam, Germany
[7]Department of Earth System Sciences, University of Hamburg, Hamburg, Germany
[8]Department of Geosciences and Natural Resource Management, University of Copenhagen, Copenhagen, Denmark
[9]School of Forest Sciences, Faculty of Science, Forestry and Technology, University of Eastern Finland, Kuopio, Finland

Correspondence: Tamara Emmerichs (tamara.emmerichs@mpimet.mpg.de)

Abstract. Although shrubs employ distinct water- and carbon-use strategies compared to trees and are increasingly expanding across warming tundra and grassland, they remain insufficiently represented in global land surface models. Here, we incorporated two shrub types, deciduous and evergreen, into the nutrient-enabled terrestrial biosphere model QUINCY, which features a state-of-the-art treatment of soil nutrient dynamics and carbon exchange. We investigate the change in C fluxes and storage due to shrub cover, it's response to climate and CO_2 fertilization effect and the role of nitrogen availability.

With this new implementation, shrubs showed reasonable seasonal cycle of gross primary production (GPP) at 50 % of the Arctic study sites. The model achieved mean R^2 values of 0.5 and 0.6, when compared with in situ measurements and remote sensing products for modeled shrubs. However, at 50 % of the study sites the model underestimated observed GPP due to too strong simulated nitrogen limitation. Compared to needle leaved evergreen forest the modeled gross primary production of shrubs is similarly distributed with a non-significant difference in the median. Compared to graminoids the carbon fluxes of shrubs are 40% higher. Shrubs produce a substantial, though lower, above-ground biomass than needle leaved trees and show phenological patterns that are distinct from those of trees. Although CO_2 fertilization generally benefits all plant types, shrubs appear to maintain a particularly strong growth response under elevated CO_2 concentrations.

We also demonstrated that the modeled deciduous shrubs reduce their nitrogen sources substantially more than evergreen shrubs, generally resulting in a 50% decrease in gross primary production. Providing the plants with unlimited nitrogen and thus doubling gross primary production at most sites improved the model-measurement agreement by 15 %. A similar effect occurred when initializing nitrogen and carbon contents best on permafrost profiles, resulting in partly alleviating nitrogen limitation in the model. These finding underlines the importance of including evergreen and deciduous shrub PFTs in global land surface models to accurately predict ongoing changes in the Arctic C cycle. However, the strong nitrogen limitation of

https://doi.org/10.5194/egusphere-2026-1514
Preprint. Discussion started: 24 March 2026

Arctic shrub productivity when using the standard model parametrizations suggests that the Arctic contribution to global land carbon is underestimated by global models.

1 Introduction

The high latitude ecosystems north of 60 degree N are vulnerable to climate change, with this region identified to be warming at around 3-fold the global rate (Giesse et al., 2024). Arctic soils store vast amounts of organic carbon (C) in continuously frozen soil layers called permafrost soils. This carbon could be released to the atmosphere as carbon dioxide or methane under climate warming and the thawing of permafrost, inducing a positive climate feedback (Schuur et al., 2015, 2022). With the increase of atmospheric temperature, prolongation of the growing season and the deepening of the active layer is causing major vegetation growth and cover shifts in the Arctic (Mekonnen et al. (2021) and references there in), Liu et al. (2025)).

Arctic shrub vegetation is short statue (mostly < 2 m tall) and often prostrate and can grow beyond the cold limits of trees due to their adaption to cold environments. Importantly, shrubs show a faster wood production than trees and thus only need a 20-50 % shorter growing seasons (Treml et al., 2019; Körner, 2012), which is a key adaptation to the Arctic conditions, and intense competition for limited light and nutrients beyond the treeline. Shrubs are classified as either evergreen and deciduous species. Deciduous shrubs grow faster than evergreen species, since their small leaf mass per unit area enables them to intercept more light for a given investment of leaf C than evergreen shrubs (Parker et al., 2021; Mekonnen et al., 2018).

Heijmans et al. (2022) found that shrubs are increasingly dominant in the Arctic. Current estimates suggest they comprise about 40 % of the Polar Arctic's plant biomass (Orndahl et al., 2025). The expansion rate has been estimated to about 38 % from 1982-2014 and 27 % from 2000-2020 in the high-northern latitudes due to increases biomass of existing stands and new establishment (Chen et al., 2020; Andreu-Hayles et al., 2020; Gui et al., 2025). Studies (Meyer et al., 2021; Elmendorf et al., 2012, e.g.), mainly report an enhanced coverage of tall deciduous shrubs such as birch, willow and alder, which is often termed as 'shrubification'. Recently, expansion of evergreen dwarf shrubs, which are ecologically different from tall deciduous shrub species, also have been observed in the Arctic (Vowles and Bjoerk, 2019). These vegetation changes are, however, spatially heterogeneous and controlled by a mixture of environmental factors other than temperature such as changes in soil wetness and plant-plant interactions (García Criado et al., 2025; Martin et al., 2022). Shrubs responding more to warming than e.g. graminoids is linked to their ability to grow their woody tissue and thereby increase their height and width of their canopy (Bret-Harte et al., 2001, 2002).

Changes in the Arctic vegetation cover initiate several feedbacks to the atmosphere by decreasing the albedo and thus rising surface temperature, and by impacting soil-plant interactions through e.g. deepening the active layer, higher mineralization rates and litter quality, which in turn affect the ecosystem's C balance (Bonfils et al., 2012; Meyer et al., 2021; Mekonnen et al., 2021). Moreover, Arctic vegetation shifts potentially affect permafrost thaw by altering the surface temperature (Heijmans

https://doi.org/10.5194/egusphere-2026-1514
Preprint. Discussion started: 24 March 2026

et al., 2022). Buckeridge et al. (2010) conclude that increased nutrient inputs via enhanced litter inputs from smaller shrub species subsequently cause an increase in growth of tall shrub tundra species.

Field studies show that shrubs have various impacts on soil nutrient cycling since they are associated with higher leaf litter quality and quantity, thus contain more nitrogen which enhances decomposition rates (Martin et al. (2022); Moore et al. (2024) and references therein) compared to Boreal trees. The vertical distribution of soil C is determined by the nutrition allocation, litter quality and plants root depth, i.e. shrubs store more C in deep soils than graminoides (Du et al., 2024). However, the effect of shrub encouragement can not only largely change with climate. The acceleration of nutrient cycling driven by higher soil temperatures and greater litter inputs and turnover, has been found to be a key player for vegetation change. However, despite the importance of these processes the impact of nutrient dynamics on shrub growth and C cycling is neglected in most commonly used vegetation models (Miller and Smith, 2012).

The magnitude of the impact of the rapid shrub expansion in Arctic landscapes on the current and future Arctic C balance is uncertain. Given the importance of shrubs in Arctic landscapes shrub plant functional types (PFTs) must be included in land biosphere models to more accurately represent C dynamics in the heterogeneous Arctic landscapes. Accordingly, we here employ the terrestrial biosphere model QUINCY (QUantifying Interactions between terrestrial Nutrient CYcles and the climate system v1.0) (Thum et al., 2020) which includes the main features of Arctic ecosystems such as soil C storage, nutrient limitation and vertical discretization for a realistic simulation of C dynamics in the Arctic and physical processes relevant in high latitudes (Lacroix et al., 2022). In contrast to other major community land models, QUINCY represents vegetation with PFTs based on physiology and not on geography which overcomes regional PFT definitions like boreal trees, thus limiting the need for parameters to a minimum (Thum et al., 2020). To assess the effects of shrub expansion for ecosystem C dynamics across the Arctic, we here implemented two shrub PFTs firstly into QUINCY (Sec.2.1, 2.3). With this new model configuration, we performed simulations taking into account coverage by three different vegetation types, namely boreal forest, graminoids and shrubs from 16 Arctic sites. Additionally, we conducted sensitivity simulations with constant CO_2, with nitrogen supply set to levels that do not limit carbon cycling and with nutrient initialization in the permafrost (Sec. 2.2), respectively. By the means of this simulations and two observational datasets (Sec. 2.4) we aimed to answer the following research specific questions:

(1) How much carbon do shrubs take up and store and is this in agreement with observations? - Section 3.1

(2) How does the response of C uptake and storage in shrub covered ecosystems to combined climate warming and CO_2 fertilization differ from boreal forest and graminoid-dominated tundra? - Section 3.2 and 3.2.1

(3) What role does nitrogen cycling play for shrub growth and C storage, in particular in response to increasing nitrogen availability from permafrost thaw? - Section 3.3

2 Methods

2.1 QUINCY model

The terrestrial biosphere model QUINCY (Thum et al., 2020; qui, 2019) simulates the coupled C, nitrogen (N) and phosphorus (P) as well as water and energy cycles. The model represents physical processes relevant to high latitudes, such as snow

https://doi.org/10.5194/egusphere-2026-1514
Preprint. Discussion started: 24 March 2026

dynamics, soil freeze-thaw, and adaptive rooting depth to layers that are non-frozen (Lacroix et al., 2022). The standard version of the model includes 12 different PFTs with flexible parametrizations for leaf characteristics, phenology and other growth and turnover dynamics. This concept of PFTs groups all plant species in a limited number of classes and thus allows a much more traceable interpretation of the plant's interactions (Poulter et al., 2015). The about 40 parameterizations representing the different plant characteristics and functionalities in QUINCY are based on plant trait databases (KATTGE et al.). Here, we added additional PFTs to simulate Arctic shrubs.

In QUINCY, vegetation consist of structural pools (leaves, sapwood, heartwood, coarse roots, fine roots, and fruit), a fast overturning, respiring non-structural pool (labile), as well as a seasonal, non-respiring, and non-structural storage pool (reserve). The canopy has several layers (multilayer canopy scheme), which includes a representation of photosynthesis and canopy conductance for sunlit and shaded leaves separately within every layer. Vegetation processes as well as nutrient uptake and availability respond to local environmental conditions on a process-specific time scale, dynamically enabling a certain memory effect (Thum et al., 2020). Plants partition the required C between growth, respiration and storage, with acclimation to meteorological conditions and nutrient availability.

The soil is explicitly vertically-discretized in 15 layers with increasing thickness down to a depth of 9.5 m. This applies for soil temperature, texture, moisture and the biogeochemical soil pools. Soil biogeochemical pools are represented by five organic pools: structural, polymeric, and woody litter, fast and slow degrading soil organic matter; as well as solute concentrations of ammonium (NH_4), nitrate (NO_3) and phosphorus (PO_4). Each of these organic pools contains C, N and P (Thum et al., 2020). In particular, the model accounts for the full nitrogen cycle in the soil, simulating nitrogen inputs through symbiotic (microbial) fixation at higher plants and free-living (asymbiotic) N fixation at all parts of the ecosystem, N deposition, and the transformation processes mineralization, nitrification and denitrification, as well as transport between soil layers. N is always accounted for as NO_3^- and NH_4^+.

2.2 Site-level simulations setup and forcings

Site-level QUINCY model simulations were conducted for 16 Arctic sites (Fig. A1, Table A1) from 1901 to 2010 where data measured at shrubs and GPP estimates were provided by the ABCflux dataset version 2. In the reference simulation, we represent the vegetation at the 16 sites by one of the two shrub PFTs according to the reported vegetation at the sites (Table A2). The simulations include nitrogen dynamics since plants in the Arctic are known to be often limited by mineral nitrogen (Mekonnen et al., 2018; Martin et al., 2017; Prager et al., 2017). Different model configurations were chosen to quantify the differences towards ecosystems covered by gramomids and NE trees at the same sites. A second set of simulations disentangle between effects caused by climate drivers, CO_2 fertilization and nutrient limitation (1).

The standard initialization of QUINCY does not account for the elevated contents of soil organic C & N characteristic to permafrost soils. These contents can also not be built up in a standard QUINCY spin-up, as they would require a paleo-timescale type simulation reproducing (at least) the last interglacial and glacial, which is neither practical for our applications, nor do the required model forcing data exist. In this study, we therefore changed the initialization procedure by adapting both C and N contents as well as the distribution of the initialization in the case a site is identified as permafrost based on the

https://doi.org/10.5194/egusphere-2026-1514
Preprint. Discussion started: 24 March 2026

definition by Palmtag et al. (2022). The distribution curve in the permafrost is initialized with a Weibull function assuming a shape parameter of 0.6 (instead of 2) according to Palmtag et al. (2022). A minimum relative deep permafrost concentration is set to 0.3 of surface soil concentrations according to estimated distributions from Palmtag et al. (2022). The soil organic matter is initialized with a single permafrost content of 121000 gC m-2 yr-1 for the first 3 m, which is the vertically-integrated average C estimated by Palmtag et al. (2022). The permafrost nitrogen is initialized using a C:N ratio of 14 according to Palmtag et al. (2022). We note that the applied approach does not account for spatial heterogeneity in permafrost soil contents and distributions for initialization.

The meteorological forcing driving the model stems from the University of East Anglia Climatic Research Unit Japanese Reanalysis (CRU-JRA; Harris (2019)), which is a reanalysis of incoming solar radiation, surface temperature, humidity, precipitation, surface pressure, and surface winds. The dataset is available at a spatial resolution of 0.5×0.5 degrees and at a 6-hourly temporal resolution. The data for our selected sites were extracted from the CRU-JRA dataset according to their geographic coordinates (Zaehle and Friend, 2010). Furthermore, the soil is represented by 15 layers, with increasing thickness down to a depth of 9.5 m. The model starts the transient simulations after a spin-up period of 1000 years using repeating forcing data from 1901-1930. The atmospheric CO_2 concentrations are prescribed according to Friedlingstein et al. (2022).

Table 1. Description of the conducted simulations (1901-2010)

Simulation	PFT	Forcing	Nutrients
Shrubs	shrub PFTs	atmospheric CO_2 forcing according to Friedlingstein et al. (2022)	C and N dynamics (CN mode)
Trees	needle-leaf evergreen	atmospheric CO_2 forcing according to Friedlingstein et al. (2022)	C and N dynamics (CN mode)
Grass	C_3 graminoid (TeH)	atmospheric CO_2 forcing according to Friedlingstein et al. (2022)	C and N dynamics (CN mode)
ShrubsNOf	shrub PFTs	constant CO_2	C and N dynamics (CN mode)
TreesNOf	NE trees	constant CO_2	C and N dynamics (CN mode)
GrassNOf	C_3 graminoid	constant CO_2	C and N dynamics (CN mode)
ShrubsConly	shrub PFTs	atmospheric CO_2 forcing according to Friedlingstein et al. (2022)	C (C-only)
ShrubsNfertC	shrub PFTs	constant CO_2	C (C-only)
ShrubsPM	shrub PFTs	atmospheric CO_2 forcing according to Friedlingstein et al. (2022)	C and N dynamics (CN mode), addition of permafrost nutrients

2.3 New shrub implementation

We implemented two new shrub PFTs: broadleaved deciduous (BD) and needle-leaved evergreen (NE). As a baseline, the two shrubs are similarly parametrized as trees but treat important aspects concerning the initial leaf N, plant allometry, root distribution and turnover times of wood differently. The new parameters are listed in Table 2. According to the physiological and phenological differences to trees (heartwood development, leaf/sapwood ratio, growing, turnover, leaf nitrogen, roots) new parameters were specified differently to the default BD and NE PFT, respectively, based on measurement studies and trait databases (e.g. TRY).

https://doi.org/10.5194/egusphere-2026-1514
Preprint. Discussion started: 24 March 2026

Table 2. New parameters for NE and BD shrubs replacing the default needle-leaved evergreen PFT. For simplicity, the latter one is referred to as 'Tree'.

Parameter	BD default (Trees)	BD shrub	NE default (Trees)	NE shrub	Reference
Default leaf nitrogen concentration ($Leaf_N$ in [mgN gDW-1])	21.34	23.43	12.09	10.11	TRY database KATTGE et al.
Turnover time of the fraction of sapwood that is in branches (τ_{branch} in [years])	10	40	10	30	based on higher sapwood
Turnover time of the fraction of sapwood that is in branches ($\tau_{sapwood}$ in [years])	40	70	40	60	Zhang et al. (2013)
Fraction of sapwood that is in branches, sapwood that is turned to litter ($frac_{sapwood-branch}$)	0.05	0.1	0.05	0.02	Thum et al. (2020)
Parameter in height diameter relationship ($allom_{k1}$)	55	35	55	25	Zhang et al. (2013)
Parameter defining the root distribution ($k_{root,dist}$)	2.0	3.5	2.0	3.5	
Leaf area to sapwood area ratio (k_{latosa})	4000	3500	4000	3500	Zhang et al. (2013); He et al. (2025)
Coarse root to sapwood mass ratio (k_{crtos}	0.1	0.9	0.1	0.9	Ma et al. (2021)
Weekly air temperature threshold ($t_{air,senescence}$ in [degC])	8.5	0	0	0	Fu et al. (2014)
Maximum GDD requirement ($gdd_{req,max}$ in [degC days])	800	34.8	0	0	Fu et al. (2014) and courtesy to Yu Zhu
Scaling factor in the GDD for dormancy ($k_{gdd,dormance}$ in [days -1])	0.007	0	0	0	Fu et al. (2014)

2.4 Observational data

The ABCfluxnet v2 (Virkkala et al., 2025b; Leffler et al., 2026) data was recently compiled to provide a dataset of in-situ Arctic–boreal terrestrial ecosystem CO_2 flux measurements (Virkkala et al., 2025a). The synthesized GPP is given as cumulative flux densities aggregated at the monthly timescale. In addition to eddy covariance data, this includes fluxes estimated with chamber methods to increase data coverage, which were performed during the growing season. We selected sites where the growth of shrubs is reported for more then one point in time. The measurements were averaged and evaluated over different years to minimize the impacts of climate variability. First, we compare our model results to the eddy-covariance (EC) data of the given site (if available) which generally represents a 100 m radius footprint of the measurement tower. The chamber data (Table A2) can be seen as a highest-resolved, plot-scale GPP estimate of a specific vegetation/soil unit.

To further evaluate the simulated GPP we also use data extracted from the global MODIS/Terra Level-4 products of MOD17A2H (collection 6) (Running et al., 2015) and MOD17A2HGF (collection 6.1) (Running and Zhao, 2021) at the site coordinates. Both products provide cumulative 8-day composite of GPP values at 500 m spatial resolution and were interpolated. They estimate GPP by applying radiation-use efficiency framework that integrates absorbed photosynthetically active radiation (APAR) with the biome-specific radiation conversion efficiency (ε) constrained by meteorological stress. While the MOD17A2H product contains gaps due to input quality, MOD17A2HGF reduces data gaps by employing additional temporal gap-filling based on quality control flags. Both products are subject to uncertainties related to input data quality, land cover classification, and model assumptions. With spatially and temporally more continuous GPP time series, the MOD17A2HGF dataset further introduces interpolation uncertainty which dampens the signals caused by inter-annual variability of climate or ecosystem disturbances. Extensive validations against eddy covariance measurements show that MOD17-series products can moderately capture the inter-annual and seasonal variability of GPP with R^2 over 0.6 across different biomes and climate regimes (Zhu et al., 2018; Tang et al., 2015; Wang et al., 2017). We extracted GPP time series from the datasets for the different sites using the nearest neighbor approach.

https://doi.org/10.5194/egusphere-2026-1514
Preprint. Discussion started: 24 March 2026

3 Results and Discussion

3.1 Modeled vegetation productivity versus observations

Comparison of the seasonal cycle of modeled and measured GPP show that the CN model configuration agrees well with the GPP measurements at around half of the sites but leads to an underestimation (R^2<0.6, Table A3), Figure 1) at the remaining sites, where the N limitation may be too strong in the CN model. The C-only model, which allows for unlimited biological N fixation, improves the model performance by 23 % with regards to the measured GPP data, in particular for NE shrubs (Fig. 1) while at three sites (XHE, SIL, IMN sites), the model's GPP estimates fall substantially below observed values. For further evaluation, we compared our model GPP outputs to GPP MODIS satellite products. MODIS data is widely used for the evaluation of the C cycle in global terrestrial biosphere models and in the Coupled Model Intercomparison Project (CMIP) models (50 % using the JSBACH surface scheme) (Hu et al., 2022), showing a high agreement in the high latitudes. Lacroix et al. (2022) reports similar correlations when comparing a permafrost-enabled version of the QUINCY model with MODIS and eddy-covariance data. Here, the MODIS GPP products show a higher correlation towards the model with a mean R^2 value of 0.62 and 0.67 (CN and C-only, Table A3) than compared to the observational data (0.48, 0.57). The MODIS products are generally in line with the observational data but they disagree significantly at two sites. At the ISK site (Norway), MODIS and (CN) model GPP agrees quite well while the observed GPP is much larger. This may be due to by the specifics of local climate and landscape at the used site coordinates. Namely, half of the field measurements at the ISK site are taken in wet tundra areas (Pirk et al., 2024) whereas the model soil hydrology tends to be rather dry (Fig.S1). A similar uncertainty source exists for the comparison at the SIL site (Finland) where most of the measurements happened in a fen ecosystem (reported in dataset as bawld-class) which is not represented in the QUINCY model. At sites with a significant fraction of forest e.g. the LET (Finland) site (Heydel and Tackenberg, 2017) both observational datasets show a higher GPP which the model does not reflect because it represents shrubs only (in this simulation). A further source of the model bias might be the underestimation of soil moisture at sites with a higher wetness than 25 % like at the Stordalen (STR, Sweden) site (Holmes et al., 2022). While we deem the agreement between model and observations inferred from field data measurements (EC measurements if available) and MODIS products to be adequate, the performance depends on the model configuration chosen, the shrub PFT type evaluated, local heterogeneity of vegetation coverage, as well as the local meteorological conditions, which may differ from the forcings used in the model.

3.2 Present day C uptake and storage

The simulated (multi-site) average annual GPP flux at shrubs is 371 gC m-2 year-1 ranging from 132 to 735 gC m-2 year-1 among the sites for the time period 1990-2010 (Fig. 2a). These estimates (and their partitioning) are in line with data synthesized by Virkkala et al. (2025a) who report an average (area-upscaled) Arctic GPP of 300 gC m-2 year-1 for tundra and 416 gC m-2 year-1 for the arctic permafrost region, albeit accounting for all tundra vegetation species (graminoids, shrubs, mosses and lichen). The distribution of annual mean GPP (Fig. 2b) overlaps with the one by the tree PFT but, in contrast, it is skewed towards higher values which shows the better adaptation of shrubs to the cold Arctic climate as it has been observed

https://doi.org/10.5194/egusphere-2026-1514
Preprint. Discussion started: 24 March 2026

Figure 1. Multi-year mean seasonal cycle of GPP [gC m-2 month-1] by measurements (field data and MODIS satellite data: MOD17A2HGF and MODIS17A2H) and model versions CN and C-only for individual time periods where field data is available. See Table A1 for the site acronyms.

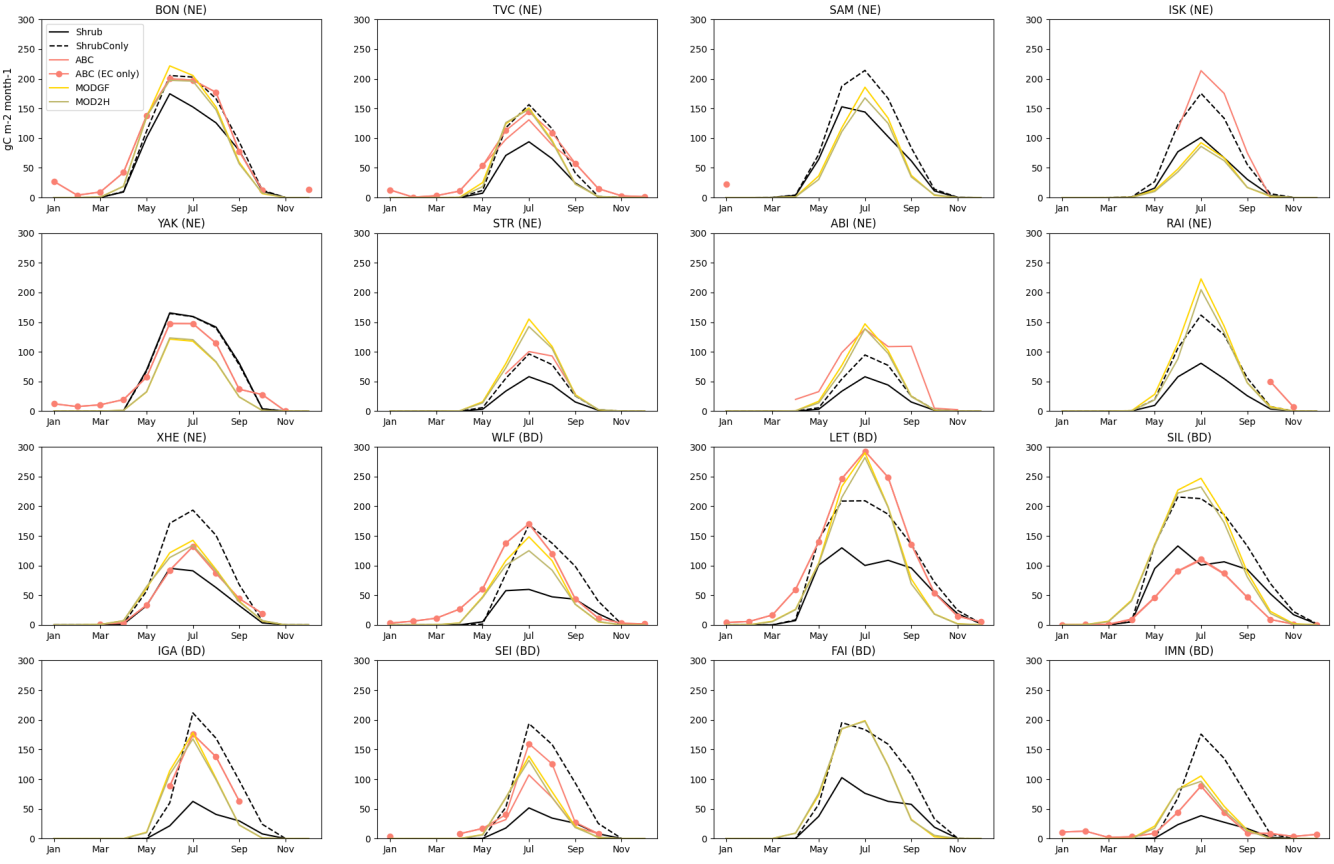

(Mekonnen et al., 2021, e.g.). Thus, the median (without considering the high values) of (new) shrub and tree PFT are not significantly different, while the average annual GPP is increased by 16 % due to the implementation of shrubs. Also, Meyer et al. (2021) report a substantial higher GPP at shrubs than at trees simulated at an site Canadian site with the CLASSIC model which is in good agreement with the site measurements. Shrubs dominance instead of graminoid cover would rise annual mean and median GPP by 40 %, respectively.

The GPP change of the three PFTs is determined by different N pathways whereas the strength of the correlation varies not only across the PFTs but also across the sites. For instance, the GPP at NE trees and shrubs increases much stronger with NH_4^+ uptake than at graminoids while comparing gramonoids and trees to BD shrubs reveals a similar slope (Fig. S2). Thus, among the shrub species, the model simulate faster growth for deciduous shrubs in response to NH_4^+ uptake as also reported by (Chen et al., 2020). For all shrubs, the change of NH_4^+ uptake explained 50-70% of the GPP change compared to trees (see R^2 in Fig. S3). For NE shrubs, N fixation and NH_4^+ net mineralization showed also significant correlation with the GPP changes

https://doi.org/10.5194/egusphere-2026-1514
Preprint. Discussion started: 24 March 2026

Figure 2. Simulated multi-year (1990-2010) annual mean GPP [gC m-2 year-1] per PFT for 16 sites (site acronyms are given in the SI Table A1) in the *Shrubs*, *Trees* and *graminoid* (grass) simulations, with the values of two most recent years marked with '+' and (b) the distribution across all sites. The first eight bars (BON-RAI) show the results at NE shrubs, the later ones at BD shrubs.

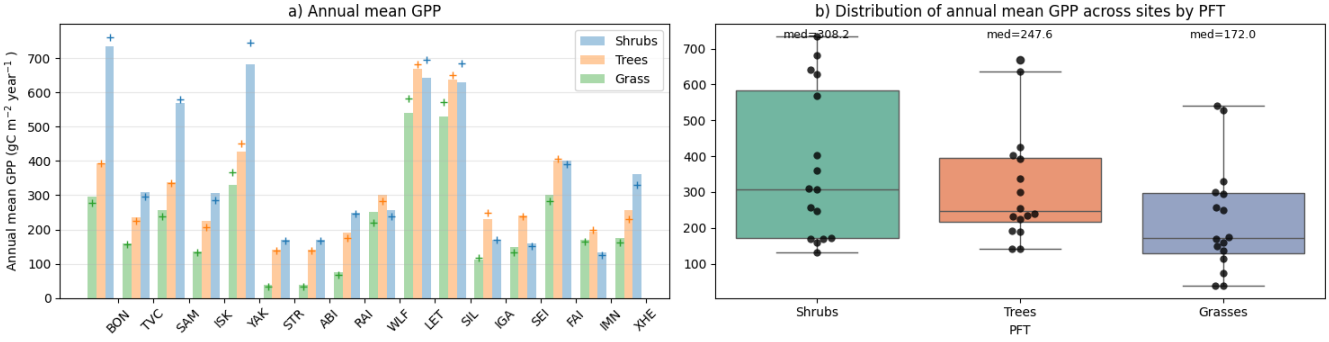

205 (Fig. S3). Most of the GPP increase at evergreen shrubs could be additionally explained by higher biological nitrogen fixation (BNF) compared to shrubs, where the absolute numbers are about half the magnitude of the plant NH_4^+ uptake (Fig. S4). Indeed, Davies-Barnard and Friedlingstein (2020) and Schore et al. (2023) report substantial higher asymbiotic BNF at shrubs than at trees driven by bacterial activity. The GPP changes at deciduous shrubs are usually lower than at evergreen shrubs which might explain the low correlation. The GPP differences from graminoids are generally less correlated to changes in the 210 N uptake pathways.

The site averaged foliage (projection) cover of shrubs, the percentage coverage of the ground area by leaves from looking down, is very similar to that of trees (4 % higher for shrubs), indicating slightly higher self-thinning in shrubs (Fig.S11).

Shrub cover reduced carbon-use efficiency (NPP/GPP), at all sites, from 0.64 (graminoid) and 0.68 (trees) to 0.63 at NE and 0.57 at BD shrubs, indicating lower efficiency in converting GPP to biomass (Fig. S7b) overall. This is generally in line with 215 satellite estimates of the NPP/GPP ratio reported by Zhang et al. (2013) for the three different vegetation types. In contrast to (needle leaved) evergreen shrubs, most deciduous shrubs had lower net primary production (NPP) than trees (Fig. S7a) following the growth respiration (Fig. S8a). A higher growth respiration would refer to a faster growth rate and higher seasonal leaf turnover (Ge et al., 2017).

The new shrub PFTs produced reasonable (aboveground) total C varying from 0.7 to 2.5 kgC m-2 (Fig. 3a, site-mean= 1.3 220 kgC m-2) in 1990-2010. Given that the aboveground part of plants contain approximately 50 % of C (Ma et al., 2018) these values translates into biomass estimates in line with measurements of 0.4-1.5 kgC m-2 (Poley et al., 2020; Zhao et al., 2021; Sulman et al., 2021; Orndahl et al., 2025).

Most of the simulated C here was stored in the living wood of the shrubs followed by the storage in coarse roots and heartwood (Fig. S6). Shrubs produced less sapwood than trees but show a faster production rate (Fig.S9) which is according to 225 (Treml et al., 2019, e.g.) explained by narrower and less xylem cells in shrubs. Therefore, deciduous shrubs grew faster than evergreen species (Figure S10) as explained (Parker et al., 2021; Mekonnen et al., 2018) by their small leaf mass per unit area enabling deciduous shrubs to intercept more light for a given investment of leaf C than evergreen shrubs. Furthermore, the

https://doi.org/10.5194/egusphere-2026-1514
Preprint. Discussion started: 24 March 2026

modeled shrubs stored more C in coarse roots than trees, so that the coarse root:sapwood ratio is increased by factor 8 which is in agreement with findings by Wang et al. (2016) and a global dataset (including 530 shrub land sites) by Ma et al. (2021). Thus, the total aboveground C storage of shrub vegetation is overall lower than in trees (at 13 out of 16 sites, Cliff's δ=-0.39). Indeed, Jobbágy and Jackson (2000) report that trees allocate more nutrients aboveground than shrubs and graminoides.

While the distribution of annual mean vegetation carbon at shrub sites overlaps with that of trees (Fig. 3a), the (multi-site) mean biomass with shrub coverage is 17 % lower than the mean tree biomass as the lower carbon use efficiency of shrubs (Fig. S7b) indicated. The shrub distribution has a much larger inter-quartile range and more skewness towards higher values than trees which pointed to the higher variability of shrubs. The total vegetation C of graminoid is significantly lower (effect size: Cliff's δ=1.0) than in both woody PFTs considering distribution, median and range as also found by Lett et al. (2004). Graminoids store relatively more C in fine root and the labile pool (almost 40%), but the size of the wood and the coarse root storage in woody plants is significantly larger.

The higher fraction of coarse root C stored by shrubs (Fig. S5a) determines the increase in total soil C, namely towards 14.3 kgC m-2 compared to the other PFTs (vs. 13.2 and 11.1 kgC m-2 multi-site annual mean at trees and graminoides) at 81 % of the stations. This small (6 %) increase of soil C due to shrub coverage compared to trees is in line with observation studies reporting more below than aboveground C with shrub vegetation coverage (Ma et al., 2021). We note that the soil type is a primary control that can explain increases as well as decreases in soil organic contents as a meta-analysis by Li et al. (2016) found at different shrub species globally. Parker et al. (2021) even report a substantial C loss by shrub expansion which is in line with other studies. At a landscape scale, Zhao et al. (2023) found an increase of soil organic carbon with shrub expansion in the Arctic. Our model study shows that, evergreen shrubs have the tendency to conserve more C than deciduous shrubs (first 8 bars in Figs. 3) as is also reported by Mekonnen et al. (2018). In comparison with graminoids, soil C is increased by 18 % as substantially more C is stored in coarse roots. Since the model does not consider the long-term C storage in permafrost soils yet the impact on soil C is only discussed briefly here. Given that shrubs exhibit higher root nutrient absorption rates than trees—supported by Chen et al. (2020), who analyzed 170 root samples from Arctic shrubs, and corroborated by our simulations (Fig. S10) significant impacts on nitrogen cycling can also be expected (Martin et al., 2022). Overall, we show here that the newly modeled shrubs produce reasonable C fluxes and storage whereas they reproduce important physiological processes (e.g. wood formation, root allocation) different from trees.

3.2.1 Transient changes in uptake and storage

Our transient simulations from 1901-2010 show an average change in annual GPP of 60 g m-2 yr-1 for shrubs, strongly increasing since 1960 (Fig. 4a). In comparison, the GPP increase over time for trees and graminoids is 30-50 % weaker.

We deduct from the *Shrubs* and *ShrubsNof* simulations the CO_2 fertilization effect on shrub GPP across the study sites, with a steep rise in the CO_2 effect on GPP since the 1960s (Fig. 4c) following increased atmospheric CO_2 concentrations (Fig. S12) (ipc, 2022). This effect is larger for sites where nitrogen dynamics have no low impact. For instance, at YAK (Yakutsk, Russia), where no difference is simulated between C-only and CN simulations, we found an GPP increase of up to 40 gC m-2 yr-1, caused by CO_2 fertilization alone. Most shrub-dominated sites are strongly nitrogen-limited, which causes the CO_2-

https://doi.org/10.5194/egusphere-2026-1514
Preprint. Discussion started: 24 March 2026

Figure 3. Multi-year (1990-2010) annual mean total vegetation C , values of two most recent years marked with '+' and (b) distribution of multi-year annual mean total soil C per PFT in [kgC m-2]. The first eight bars (BON-RAI) show the results of NE shrubs, the later ones of BD shrubs.

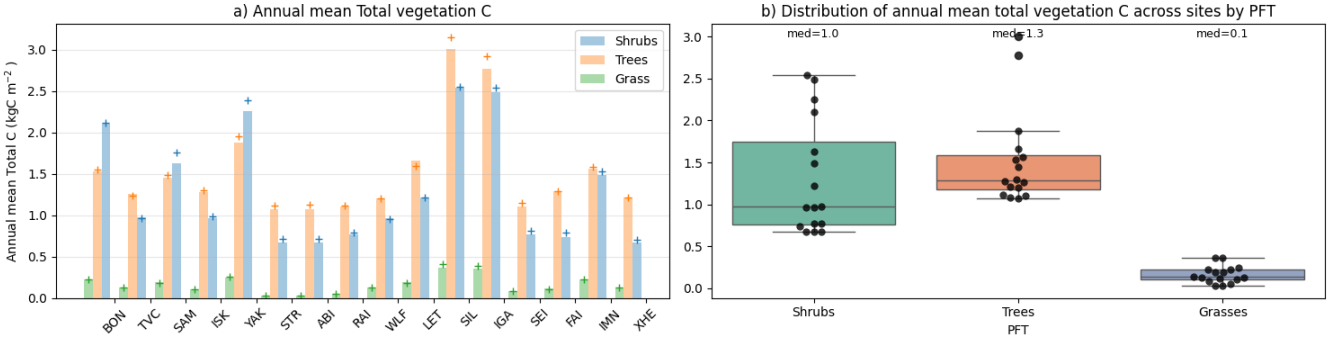

fertilization effect to be small on average (Fig.4a) across all sites for 1960-2010. This estimate is in line with the QUINCY model study results for the high-Arctic tundra by Lacroix et al. (2022), as well as with a number of field N fertilization experiments with tundra and mixed shrub coverage (DeMarco et al., 2014; Shaver et al., 2001). For NE trees, positive changes in GPP outweigh negative changes at only a few sites over time leading to an overall small change (Fig.4a), consistent with their lower N uptake compared to shrubs. Thus, the newly modeled shrubs show a higher growing potential (N uptake, GPP) under increased CO_2 in comparison to NE trees (default parameters). The CO_2-fertilization effect (on GPP) is higher the less the sites are nitrogen-limited (e.g. the YAK site, Russia). Indeed shrubs have been found to deepen their roots in response to increasing CO_2 (Mekonnen et al., 2021).

After 1960, the climate effect clearly becomes dominating due to the strong temperature increase in the Arctic as e.g. reported by Wei et al. (2018). The multi-site average GPP increases until 45 gC m-2 yr-1 at shrub-dominated sites relative to 1901-1910, which is about 12 % of the absolute GPP. For trees, the foilage projection cover rise similarly over time as for shrubs (Fig.2), while the GPP at graminoids show approximately half of the increase. Until 1960, the climate impact of all three PFTs exhibits a 20-year cycle, driven by variations in dominant climate factors. Overall, among all three PFTs shrubs respond most to climate effects in the model, e.g. increasing temperature (since 1960). This feature is reported as reason for the shrub expansion in the Arctic as described in Mekonnen et al. (2021, e.g.,).

Unsurprisingly, alleviating N limitation in the (*ShrubsConly*, *ShrubsNOf*) simulations result in a substantially higher CO_2 fertilization effect (on average 58 gC m2 year-1, Fig. 4b). This can be explained by the change in (plant) biological nitrogen fixation (BNF) during unlimited N supply. BNF rises with increasing temperature (Yu and Zhuang, 2020) and the model formulation used here favors elevated CO_2 (Meyerholt et al., 2016). Thus, here BNF increases with rising CO_2 by 5 % yr-1 (Fig. S14), so that 2010 the CO_2 fertilized C-only simulation reached 30 % more BNF than the non-fertilized simulation. BNF is known an important N source for plants, whereas the contribution of symbiotic (bacteria) and free-living parts is uncertain (Davies-Barnard et al., 2020). In our C-only model used here plant BNF is unlimited. Thus, a simulation estimate twice the

https://doi.org/10.5194/egusphere-2026-1514
Preprint. Discussion started: 24 March 2026

Figure 4. Multi sites average 15-years rolling mean total changes (a,b) and CO_2 fertilization and climate effect (c,d) in GPP relative to 1901-1911 [gC m-2 yr-1] carried out with the N dynamic and C-only model configuration, respectively.

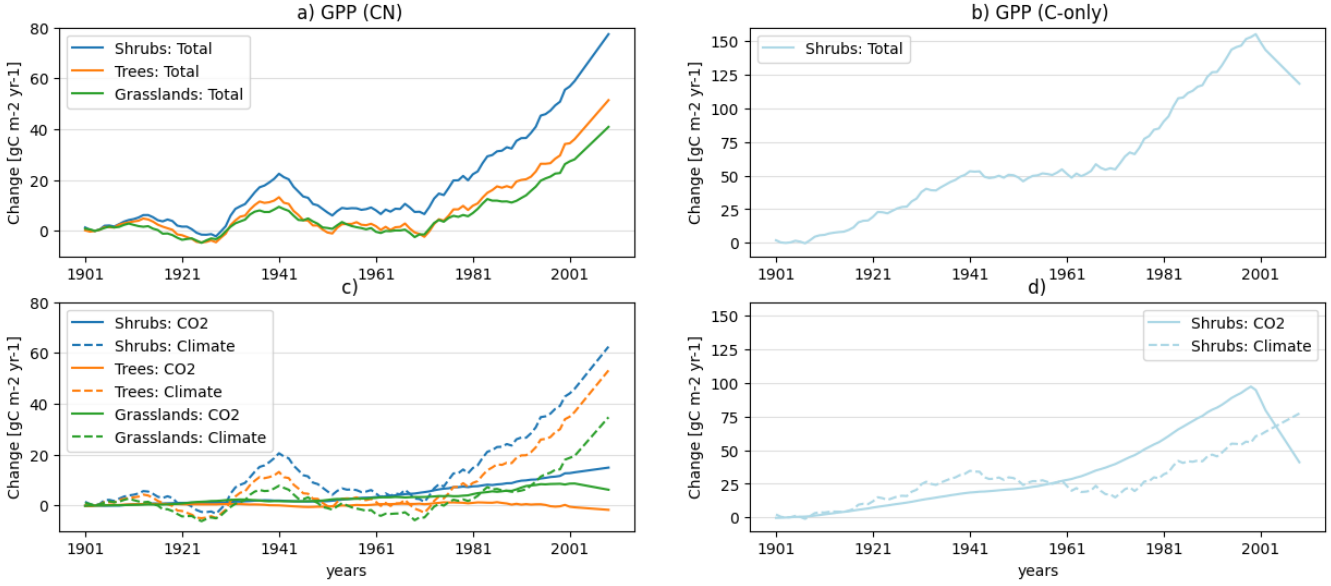

observations in the Arctic (see Meyerholt et al. (2016)) compensates for missing N sources (like symbiotic BNF, gray line in Fig. S14).

The climate effect on total vegetation C (Fig.S13) is similar as for GPP with a sharp increase around 1970 to a change of 0.2 kgC m-2 (8% of the absolute) at shrubs. In fact, many studies like Elmendorf et al. (2012) report the boost in Arctic ecosystem productivity due to climate warming. The CO_2 fertilization, however, is minor at shrubs and graminoids while it even leads to a reduction in tree vegetation C of about 5 %. Comparing the CN and C-only simulations of shrubs reveal the same climate effect as the climate forcing is the same but a much higher CO_2 fertilization effect (0.5 kg m-2, 25 %) occurred in the C-only simulation. Norby et al. (2010) and McCarthy et al. (2010) confirm that local N availability strongly drives the strength and the sign of the CO_2 fertilization effect at Arctic trees. The change in vegetation C also reflects to the foilage projection cover of trees and shrubs. CO_2 fertilization has no significant impact on modeled shrub foliage projection cover (Fig. S11). For trees, however, we see a decrease in foilage cover when accounting for CO_2 fertilization over the last 20 simulation years (Fig. S11, orange compared to coral line) which translates into a higher self-thinning and thus a reduction of trees per leaf areas. Graminoids similarly to shrubs show only a modest CO_2 fertilization response as also seen for GPP (Fig.4a).

3.3 Role of nitrogen availability

Here, we compare the C-only (*ShrubsConly*) and CN simulations (*Shrubs*), i.e. simulations with nitrogen supply maintained at levels that do not constrain plant growth versus an explicit simulation of nitrogen input and output processes and the limitation of plant growth due to nitrogen availability. Accounting for nitrogen limitation significantly reduced the GPP at all sites in

https://doi.org/10.5194/egusphere-2026-1514
Preprint. Discussion started: 24 March 2026

Figure 5. Multi-year (1990-2010) average seasonal cycle of (a) growing season length, (b) GPP change (*Shrubs-ShrubsConly*), (c) change of N uptake and net mineralization, including NH_4^+ and NO_3- (*Shrubs-ShrubsConly*) at particular stations.

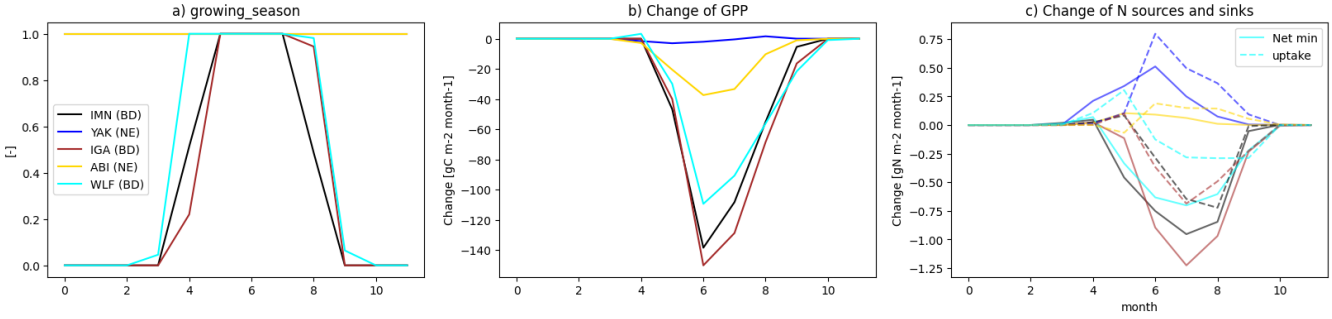

shrub cover simulations (Fig. 1, 6), most significantly at deciduous shrubs. These reductions range from 3 gC month-1 m-2 (2 %, not significant) for the evergreen shrub at the YAK site (Russia) to 150 gC month-1 m-2 (75 %) for the deciduous shrub at the IGA site in Russia (Fig. 5a). We demonstrate that the magnitude of GPP change (Fig. 5b) depends on the growing season length (Fig. 5a), which impacts the ecosystem's nitrogen supply through net N mineralization, fixation (not shown) and uptake (Fig. 5c). At sites with deciduous shrubs and a 3-months growing season only (at the sites SEI, IMN, IGA; whereas SEI and IGA shrubs behave very similar), these main N sources declined in the CN simulations leading to a strong reduction of GPP (Fig. 5b). Shrubs at other sites e.g. at the WLF site (Canada) showed at least an increase of N uptake under the CN configuration at the start of the growing season. When both N uptake terms and the use of N storage rise (at the sites YAK, STR, ABI whereas STR and ABI shrubs behave very similar) the reduction in GPP is only slight (Fig. 5b, c). Overall, we demonstrated that most simulated shrubs are strongly limited by nitrogen supply, consistent with other studies e.g. Street and Caldararu (2022). Other than evergreen shrubs, the modeled deciduous shrubs have a higher N demand and respond more rapidly to N additions as also reported for al pine shrubs by Zhou et al. (2023). However, our results suggest that the N dynamics in the model may be overly restrictive, and could be improved by refining key processes such as BNF to better reflect Arctic conditions.

The initialization of N and C in the permafrost (simulation: *ShrubsPM)* increased the soil C pool by 10-60 kgC m-2 (Fig. 6a, 4-18 %) towards a better agreement with the permafrost C estimates of 20-150 kgC m-2 (0-3 m) by (Hugelius et al., 2014) where the majority of the soil C is stored in the model. It also improves total soil N contents from 1.5 kgN m-2 to 7.4 kgN m-2 (Fig. S16). Palmtag et al. (2022) report estimates of around 5 kgN m-2, when extrapolated to our modeled soil depths of 9 m using the same vertical distribution.

The higher soil N levels originating from the improved soil initialization stimulated primary productivity, which in turn increased vegetation C storage in the coarse root, sapwood and heart wood pools of the plants. As a result, total vegetation C rose by 1 kgC m-2 (93 %) on average (Fig. S15).

For most of the sites with NE shrubs, the effects of enhanced soil N supply (Fig. S17) are strongly reflected in the annual GPP, which increased by 73-290 gC m-2 yr-1 compared to the standard model simulations (*Shrubs*). The additional nutrients lead to a significant increase of the leaf to root mass ratio (Fig. S18), clearly indicating a significant alleviation of nitrogen limitation,

https://doi.org/10.5194/egusphere-2026-1514
Preprint. Discussion started: 24 March 2026

Figure 6. Multi-year (1990-2010) average total soil C (left) and total soil nitrogen (right) at the 16 different sites estimated by the three simulations: Shrubs, ShrubsConly and ShrubsbPM.

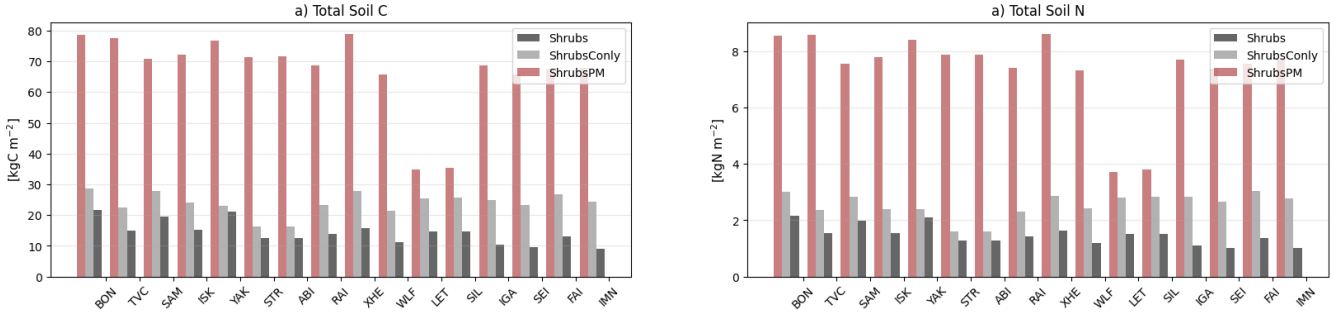

a pattern widely reported for other vegetation types, thus causing the shrubs to allocate more growth into aboveground biomass than roots, the latter is needed to take up more nutrients. In contrast, GPP for BD shrubs is less strongly affected (Fig. S17), and the leaf and fine root C ratios at BD shrub sites are also not significantly changed (Fig.S17). This feature highlights the contrasting nitrogen sensitivities and acquisition strategies of NE and BD shrubs. In fact, Martin et al. (2022) reports a rapid increase of GPP and leaf:root mass ratio at NE shrubs with higher N availability while BD shrubs only show a slight response to more N due to the conservative economics and higher respiration efficiency (Street and Caldararu, 2022).

The change in GPP due to the PM initialization varies significantly over time. From the initialization the GPP difference rapidly increases by 10 gC m-2 yr-1 to a level which is more or less constant until 1960. With increasing CO_2 the GPP difference increases by 30 gC m-2 yr-1 until 2010.

4 Conclusions

We implemented broadleaf deciduous and needle leaved evergreen shrubs into the nutrient-enabling terrestrial biosphere model QUINCY using empirically-based parameters to improve the representation of Arctic C cycle processes. We simulated shrub, tree and graminoid growth at 16 Pan-Arctic sites separately to assess the impact of Arctic shrub cover on C uptake and storage. We found that:

- Modeling shrubs using empirically-based parameters enabled a reasonable simulation of gross primary production, achieving R^2 values of 0.5–0.6 when compared with field data and MODIS satellite observations, while accurately capturing well-known physiological processes distinct from those of trees.
- At the same simulated sites, shrubs exhibit larger growth than NE forest and graminoids, leading to mean GPP increase of 16% or 40% , respectively.
- Climate-induced effects dominate over other driving factors when simulating enhanced shrub growth from 1901-2010. This is due to the nitrogen-limitation, which was strengthened with CO_2 fertilization but weakened in a warmer climate that enhanced nitrogen fixation and soil N turnover.

https://doi.org/10.5194/egusphere-2026-1514
Preprint. Discussion started: 24 March 2026

- The initialization of soil nitrogen concentrations, parametrized from observation products, enhanced shrub growth, especially at NE sites, improving the model-measurement comparison by 15 %. It also affected the increased C uptake over 1901-2010.

Overall, we show that explicitly representing shrubs significantly alters simulated C uptake and storage. This highlights the importance to incorporate both evergreen and deciduous shrub plant functional types (PFTs) in global land surface models to improve predictions on ongoing Arctic carbon cycle changes. Given the strong influence of nitrogen limitation on ecosystem C fluxes revealed here, we recommend improved constraints on soil N cycle under low-temperatures and their changes in warming climate. We also call for additional measurements needed to parametrize the PFT-specific traits, such as the allocation of biomass to roots, that influence the efficiency of shrubs in accessing soil nitrogen (Martin et al., 2022) and are likely to become increasingly important with permafrost thaw.

Code and data availability.

The code is temporary available at https://nextcloud.bgc-jena.mpg.de/s/eJjWSzMonLfLKTj for the review phase. Later, there will be a provided with a tag of the code version.

Author contributions. TE developed the shrub implementation, conducted the simulations, the analysis and the visualizations and wrote the main of the manuscript. FL importantly contributed to the concept of the manuscript, prepared the site-level model forcings and helped to set up the model. VB and FL extensively reviewed the manuscript. YZ prepared the MODIS satellite products for the model evaluation. SZ and CG did the most recent improvements of the nitrogen dynamics in QUINCY. SS, CV, KSL, EST have conducted the ABCfluxnet measurements at Stordalen, Trail Valley Creek, Abisko and Siikaneva, respectively. All authors contributed to the review of the manuscript.

Acknowledgements. TE was funded by the European Research Council under the European Union's Horizon 2020 research and innovation program as part of the Q-Arctic project (grant agreement No 951288 and by the German Research Foundation as part of the CLICCS Clusters of Excellence (DFG EXC 2037). FL received support from Swiss National Science Foundation (grant no. PZ00P2 216442). YZ was supported by the MoLiCarb project (Deutsche Forschungsgemeinschaft DFG, Project Nr. 514539694. SZ and CG were supported by the European Union's Horizon 2020 research and innovation programme under grant agreement N 101003536 (ESM-2025). CV acknowledges funding from the European Research Council Starting Grant COLDSPOT (no. 101163177). The authors acknowledge the availability of the ABCfluxnet dataset. Especially, we thank Claire Treat, Lona van Delden, Joshua Hashemi to allow using the GPP data from the Siikaneva2 chambers and Sean Carey, Erin Nicholls, Graham Clark for the tower data at Wolfs Creek.

Competing interests. The authors declare no potential conflict of interests.

https://doi.org/10.5194/egusphere-2026-1514
Preprint. Discussion started: 24 March 2026

References

Quincy Model, https://git.bgc-jena.mpg.de/quincy/quincy-model-releases, https://doi.org/10.17871/quincy-model-2019, 2019.

Emissions Trends and Drivers., IPCC, 2022: Climate Change 2022: Mitigation of Climate Change. Contribution of Working Group III to the Sixth Assessment Report of the Intergovernmental Panel on Climate Change, https://doi.org/10.1017/9781009157926.004, 2022.

Andreu-Hayles, L., Gaglioti, B. V., Berner, L. T., Levesque, M., Anchukaitis, K. J., Goetz, S. J., and D'Arrigo, R.: A narrow window of summer temperatures associated with shrub growth in Arctic Alaska, Environmental Research Letters, 15, 105 012, https://doi.org/10.1088/1748-9326/ab897f, publisher: IOP Publishing, 2020.

Bonfils, C. J. W., Phillips, T. J., Lawrence, D. M., Cameron-Smith, P., Riley, W. J., and Subin, Z. M.: On the influence of shrub height and expansion on northern high latitude climate, Environmental Research Letters, 7, 015 503, https://doi.org/10.1088/1748-9326/7/1/015503, publisher: IOP Publishing, 2012.

Bret-Harte, M. S., Shaver, G. R., Zoerner, J. P., Johnstone, J. F., Wagner, J. L., Chavez, A. S., Gunkelman, R. F., Lippert, S. C., and Laundre, J. A.: Developmental Plasticity Allows Betula nana to Dominate Tundra Subjected to an Altered Environment, Ecology, 82, 18–32, https://doi.org/10.2307/2680083, publisher: Ecological Society of America, 2001.

Bret-Harte, M. S., Shaver, G. R., and Chapin III, F. S.: Primary and secondary stem growth in arctic shrubs: implications for community response to environmental change, Journal of Ecology, 90, 251–267, https://doi.org/10.1046/j.1365-2745.2001.00657.x, _eprint: https://besjournals.onlinelibrary.wiley.com/doi/pdf/10.1046/j.1365-2745.2001.00657.x, 2002.

Buckeridge, K. M., Zufelt, E., Chu, H., and Grogan, P.: Soil nitrogen cycling rates in low arctic shrub tundra are enhanced by litter feedbacks, Plant and Soil, 330, 407–421, https://doi.org/10.1007/s11104-009-0214-8, 2010.

Chen, W., Tape, K. D., Euskirchen, E. S., Liang, S., Matos, A., Greenberg, J., and Fraterrigo, J. M.: Impacts of Arctic Shrubs on Root Traits and Belowground Nutrient Cycles Across a Northern Alaskan Climate Gradient, Frontiers in Plant Science, 11, https://doi.org/10.3389/fpls.2020.588098, publisher: Frontiers, 2020.

Davies-Barnard, T. and Friedlingstein, P.: The Global Distribution of Biological Nitrogen Fixation in Terrestrial Natural Ecosystems, Global Biogeochemical Cycles, 34, e2019GB006 387, https://doi.org/10.1029/2019GB006387, publisher: John Wiley & Sons, Ltd, 2020.

Davies-Barnard, T., Meyerholt, J., Zaehle, S., Friedlingstein, P., Brovkin, V., Fan, Y., Fisher, R. A., Jones, C. D., Lee, H., Peano, D., Smith, B., Wårlind, D., and Wiltshire, A. J.: Nitrogen cycling in CMIP6 land surface models: progress and limitations, Biogeosciences, 17, 5129–5148, https://doi.org/10.5194/bg-17-5129-2020, publisher: Copernicus GmbH, 2020.

DeMarco, J., Mack, M. C., and Bret-Harte, M. S.: Effects of arctic shrub expansion on biophysical vs. biogeochemical drivers of litter decomposition, Ecology, 95, 1861–1875, https://doi.org/10.1890/13-2221.1, publisher: John Wiley & Sons, Ltd, 2014.

Du, Z., Zheng, H., Penuelas, J., Sardans, J., Deng, D., Cai, X., Gao, D., Nie, S., He, Y., Lü, X., and Li, M.-H.: Shrub encroachment leads to accumulation of C, N, and P in grassland soils and alters C:N:P stoichiometry: A meta-analysis, Science of The Total Environment, 951, 175 534, https://doi.org/10.1016/j.scitotenv.2024.175534, 2024.

Elmendorf, S. C., Henry, G. H. R., Hollister, R. D., Bjoerk, R. G., Boulanger-Lapointe, N., Cooper, E. J., Cornelissen, J. H. C., Day, T. A., Dorrepaal, E., Elumeeva, T. G., Gill, M., Gould, W. A., Harte, J., Hik, D. S., Hofgaard, A., Johnson, D. R., Johnstone, J. F., Jónsdóttir, I. S., Jorgenson, J. C., Klanderud, K., Klein, J. A., Koh, S., Kudo, G., Lara, M., Lévesque, E., Magnússon, B., May, J. L., Mercado-Dıaz, J. A., Michelsen, A., Molau, U., Myers-Smith, I. H., Oberbauer, S. F., Onipchenko, V. G., Rixen, C., Martin Schmidt, N., Shaver, G. R., Spasojevic, M. J., Porhallsdottir, P. E., Tolvanen, A., Troxler, T., Tweedie, C. E., Villareal, S., Wahren, C.-H., Walker, X., Webber, P. J.,

https://doi.org/10.5194/egusphere-2026-1514
Preprint. Discussion started: 24 March 2026

Welker, J. M., and Wipf, S.: Plot-scale evidence of tundra vegetation change and links to recent summer warming, Nature Climate Change, 2, 453–457, https://doi.org/10.1038/nclimate1465, publisher: Nature Publishing Group, 2012.

Friedlingstein, P., O'Sullivan, M., Jones, M. W., Andrew, R. M., Gregor, L., Hauck, J., Le Quéré, C., Luijkx, I. T., Olsen, A., Peters, G. P., Peters, W., Pongratz, J., Schwingshackl, C., Sitch, S., Canadell, J. G., Ciais, P., Jackson, R. B., Alin, S. R., Alkama, R., Arneth, A., Arora, V. K., Bates, N. R., Becker, M., Bellouin, N., Bittig, H. C., Bopp, L., Chevallier, F., Chini, L. P., Cronin, M., Evans, W., Falk, S., Feely, R. A., Gasser, T., Gehlen, M., Gkritzalis, T., Gloege, L., Grassi, G., Gruber, N., Guerses, , Harris, I., Hefner, M., Houghton, R. A., Hurtt, G. C., Iida, Y., Ilyina, T., Jain, A. K., Jersild, A., Kadono, K., Kato, E., Kennedy, D., Klein Goldewijk, K., Knauer, J., Korsbakken, J. I., Landschützer, P., Lefèvre, N., Lindsay, K., Liu, J., Liu, Z., Marland, G., Mayot, N., McGrath, M. J., Metzl, N., Monacci, N. M., Munro, D. R., Nakaoka, S.-I., Niwa, Y., O'Brien, K., Ono, T., Palmer, P. I., Pan, N., Pierrot, D., Pocock, K., Poulter, B., Resplandy, L., Robertson, E., Rödenbeck, C., Rodriguez, C., Rosan, T. M., Schwinger, J., Séférian, R., Shutler, J. D., Skjelvan, I., Steinhoff, T., Sun, Q., Sutton, A. J., Sweeney, C., Takao, S., Tanhua, T., Tans, P. P., Tian, X., Tian, H., Tilbrook, B., Tsujino, H., Tubiello, F., van der Werf, G. R., Walker, A. P., Wanninkhof, R., Whitehead, C., Willstrand Wranne, A., Wright, R., Yuan, W., Yue, C., Yue, X., Zaehle, S., Zeng, J., and Zheng, B.: Global Carbon Budget 2022, Earth System Science Data, 14, 4811–4900, https://doi.org/10.5194/essd-14-4811-2022, 2022.

Fu, Y., Piao, S., Zhao, H., Jeong, S., Wang, X., Vitasse, Y., Ciais, P., and Janssens, I.: Unexpected role of winter precipitation in determining heat requirement for spring vegetation green-up at northern middle and high latitude, Global Change Biology, 20, https://doi.org/10.1111/gcb.12610, 2014.

García Criado, M., Myers-Smith, I. H., Bjorkman, A. D., Elmendorf, S. C., Normand, S., Aastrup, P., Aerts, R., Alatalo, J. M., Baeten, L., Bjoerk, R. G., Bjoerkman, M. P., Boulanger-Lapointe, N., Butler, E. E., Cooper, E. J., Cornelissen, J. H. C., Daskalova, G. N., Fadrique, B., Forbes, B. C., Henry, G. H. R., Hollister, R. D., Høye, T. T., Jacobsen, I. B. D., Jägerbrand, A. K., Jónsdóttir, I. S., Kaarlejärvi, E., Khitun, O., Klanderud, K., Kolari, T. H. M., Lang, S. I., Lecomte, N., Lenoir, J., Macek, P., Messier, J., Michelsen, A., Molau, U., Muscarella, R., Nielsen, M.-L., Petit Bon, M., Post, E., Raundrup, K., Rinnan, R., Rixen, C., Ryde, I., Serra-Diaz, J. M., Schaepman-Strub, G., Schmidt, N. M., Schrodt, F., Sjögersten, S., Steinbauer, M. J., Stewart, L., Strandberg, B., Tolvanen, A., Tweedie, C. E., and Vellend, M.: Plant diversity dynamics over space and time in a warming Arctic, Nature, 642, 653–661, https://doi.org/10.1038/s41586-025-08946-8, publisher: Nature Publishing Group, 2025.

Ge, L., Lafleur, P. M., and Humphreys, E. R.: Respiration from Soil and Ground Cover Vegetation Under Tundra Shrubs, Arctic, Antarctic, and Alpine Research, 49, 537–550, https://doi.org/10.1657/AAAR0016-064, 2017.

Giesse, C., Notz, D., and Baehr, J.: The Shifting Distribution of Arctic Daily Temperatures Under Global Warming, Earth's Future, 12, e2024EF004 961, https://doi.org/10.1029/2024EF004961, _eprint: https://onlinelibrary.wiley.com/doi/pdf/10.1029/2024EF004961, 2024.

Gui, Y., Wang, K., Huntingford, C., Wei, S., Li, X., Myneni, R. B., and Piao, S.: Vegetation greenness in 2024, Nature Reviews Earth & Environment, 6, 255–257, https://doi.org/10.1038/s43017-025-00656-z, publisher: Nature Publishing Group, 2025.

Harris, I. C.: CRU JRA v1.1: A forcings dataset of gridded land surface blend of climatic research unit (CRU) and Japanese reanalysis (JRA) data; Jan.1901—Dec.2017, 2019.

He, P., Ye, Q., Yu, K., Wang, H., Xu, H., Yin, Q., Yue, M., Liang, X., Wang, W., You, Z., Zhong, Y., and Liu, H.: Growing-Season Precipitation Is a Key Driver of Plant Leaf Area to Sapwood Area Ratio at the Global Scale, Plant, Cell & Environment, 48, 746–755, https://doi.org/10.1111/pce.15169, _eprint: https://onlinelibrary.wiley.com/doi/pdf/10.1111/pce.15169, 2025.

Heijmans, M. M. P. D., Magnusson, R. , Lara, M. J., Frost, G. V., Myers-Smith, I. H., van Huissteden, J., Jorgenson, M. T., Fedorov, A. N., Epstein, H. E., Lawrence, D. M., and Limpens, J.: Tundra vegetation change and impacts on permafrost, Nature Reviews Earth & Environment, 3, 68–84, https://doi.org/10.1038/s43017-021-00233-0, publisher: Nature Publishing Group, 2022.

https://doi.org/10.5194/egusphere-2026-1514
Preprint. Discussion started: 24 March 2026

Heydel, F. and Tackenberg, O.: How are the phenologies of ripening and seed release affected by species' ecology and evolution?, Oikos, 126, 738–747, https://doi.org/10.1111/oik.03442, _eprint: https://onlinelibrary.wiley.com/doi/pdf/10.1111/oik.03442, 2017.

Holmes, M. E., Crill, P. M., Burnett, W. C., McCalley, C. K., Wilson, R. M., Frolking, S., Chang, K.-Y., Riley, W. J., Varner, R. K., Hodgkins, S. B., Coordinators, I. P., Team, I. F., McNichol, A. P., Saleska, S. R., Rich, V. I., and Chanton, J. P.: Carbon Accumulation, Flux, and Fate in Stordalen Mire, a Permafrost Peatland in Transition, Global Biogeochemical Cycles, 36, e2021GB007 113, https://doi.org/https://doi.org/10.1029/2021GB007113, e2021GB007113 2021GB007113, 2022.

Hu, Q., Li, T., Deng, X., Wu, T., Zhai, P., Huang, D., Fan, X., Zhu, Y., Lin, Y., Xiao, X., Chen, X., Zhao, X., Wang, L., and Qin, Z.: Intercomparison of global terrestrial carbon fluxes estimated by MODIS and Earth system models, Science of The Total Environment, 810, 152 231, https://doi.org/https://doi.org/10.1016/j.scitotenv.2021.152231, 2022.

Hugelius, G., Strauss, J., Zubrzycki, S., Harden, J. W., Schuur, E. A. G., Ping, C.-L., Schirrmeister, L., Grosse, G., Michaelson, G. J., Koven, C. D., O'Donnell, J. A., Elberling, B., Mishra, U., Camill, P., Yu, Z., Palmtag, J., and Kuhry, P.: Estimated stocks of circumpolar permafrost carbon with quantified uncertainty ranges and identified data gaps, Biogeosciences, 11, 6573–6593, https://doi.org/10.5194/bg-11-6573-2014, publisher: Copernicus GmbH, 2014.

Jobbágy, E. G. and Jackson, R. B.: The Vertical Distribution of Soil Organic Carbon and Its Relation to Climate and Vegetation, Ecological Applications, 10, 423–436, https://doi.org/10.1890/1051-0761(2000)010[0423:TVDOSO]2.0.CO;2, _eprint: https://onlinelibrary.wiley.com/doi/pdf/10.1890/1051-0761%282000%29010%5B0423%3ATVDOSO%5D2.0.CO%3B2, 2000.

KATTGE, J., DÍAZ, S., LAVOREL, S., PRENTICE, I. C., LEADLEY, P., BÖNISCH, G., GARNIER, E., WESTOBY, M., REICH, P. B., WRIGHT, I. J., CORNELISSEN, J. H. C., VIOLLE, C., HARRISON, S. P., Van BODEGOM, P. M., REICHSTEIN, M., ENQUIST, B. J., SOUDZILOVSKAIA, N. A., ACKERLY, D. D., ANAND, M., ATKIN, O., BAHN, M., BAKER, T. R., BALDOCCHI, D., BEKKER, R., BLANCO, C. C., BLONDER, B., BOND, W. J., BRADSTOCK, R., BUNKER, D. E., CASANOVES, F., CAVENDER-BARES, J., CHAMBERS, J. Q., CHAPIN III, F. S., CHAVE, J., COOMES, D., CORNWELL, W. K., CRAINE, J. M., DOBRIN, B. H., DUARTE, L., DURKA, W., ELSER, J., ESSER, G., ESTIARTE, M., FAGAN, W. F., FANG, J., FERNÁNDEZ-MÉNDEZ, F., FIDELIS, A., FINEGAN, B., FLORES, O., FORD, H., FRANK, D., FRESCHET, G. T., FYLLAS, N. M., GALLAGHER, R. V., GREEN, W. A., GUTIERREZ, A. G., HICKLER, T., HIGGINS, S. I., HODGSON, J. G., JALILI, A., JANSEN, S., JOLY, C. A., KERKHOFF, A. J., KIRKUP, D., KITAJIMA, K., KLEYER, M., KLOTZ, S., KNOPS, J. M. H., KRAMER, K., KÜHN, I., KUROKAWA, H., LAUGHLIN, D., LEE, T. D., LEISHMAN, M., LENS, F., LENZ, T., LEWIS, S. L., LLOYD, J., LLUSIÀ, J., LOUAULT, F., MA, S., MAHECHA, M. D., MANNING, P., MASSAD, T., MEDLYN, B. E., MESSIER, J., MOLES, A. T., MÜLLER, S. C., NADROWSKI, K., NAEEM, S., NINEMETS, , NOELLERT, S., NÜSKE, A., OGAYA, R., OLEKSYN, J., ONIPCHENKO, V. G., ONODA, Y., ORDOÑEZ, J., OVERBECK, G., OZINGA, W. A., PATIÑO, S., PAULA, S., PAUSAS, J. G., PEÑUELAS, J., PHILLIPS, O. L., PILLAR, V., POORTER, H., POORTER, L., POSCHLOD, P., PRINZING, A., PROULX, R., RAMMIG, A., REINSCH, S., REU, B., SACK, L., SALGADO-NEGRET, B., SARDANS, J., SHIODERA, S., SHIPLEY, B., SIEFERT, A., SOSINSKI, E., SOUSSANA, J.-F., SWAINE, E., SWENSON, N., THOMPSON, K., THORNTON, P., WALDRAM, M., WEIHER, E., WHITE, M., WHITE, S., WRIGHT, S. J., YGUEL, B., ZAEHLE, S., ZANNE, A. E., and WIRTH, C.: TRY – a global database of plant traits, Global Change Biology, 17, 2905–2935, https://doi.org/https://doi.org/10.1111/j.1365-2486.2011.02451.x.

Körner, C.: Alpine Treelines: Functional Ecology of the Global High Elevation Tree Limits Springer, Basel, Google Scholar, pp. 141–173, 2012.

https://doi.org/10.5194/egusphere-2026-1514
Preprint. Discussion started: 24 March 2026

Lacroix, F., Zaehle, S., Caldararu, S., Schaller, J., Stimmler, P., Holl, D., Kutzbach, L., and Göckede, M.: Mismatch of N release from the permafrost and vegetative uptake opens pathways of increasing nitrous oxide emissions in the high Arctic, Global Change Biology, 28, 5973–5990, https://doi.org/10.1111/gcb.16345, _eprint: https://onlinelibrary.wiley.com/doi/pdf/10.1111/gcb.16345, 2022.

Leffler, A. J., Serrone, A., Bolek, A., Rocha, A. V., Korrensalo, A., Vähä, A., Tremblay, A., Barr, A., Salazar, A., Sabrekov, A. F., Rasanen, A., Mavrovic, A., Roy, A., Panov, A. V., Townsend-Small, A., Niyazova, A., Prokushkin, A., Jonsson, A., Lindroth, A., and … Harazono, Y.: ABCFlux v2: Arctic-Boreal CO2 and CH4 In-situ Flux and Environmental Data (Version 1), ORNL Distributed Active Archive Center, https://doi.org/10.3334/ORNLDAAC/2448, accessed: 2026-02-25, 2026.

Lett, M. S., Knapp, A. K., Briggs, J. M., and Blair, J. M.: Influence of shrub encroachment on aboveground net primary productivity and carbon and nitrogen pools in a mesic grassland, Canadian Journal of Botany, 82, 1363–1370, https://doi.org/10.1139/b04-088, publisher: NRC Research Press, 2004.

Li, H., Shen, H., Chen, L., Liu, T., Hu, H., Zhao, X., Zhou, L., Zhang, P., and Fang, J.: Effects of shrub encroachment on soil organic carbon in global grasslands, Scientific Reports, 6, 28 974, https://doi.org/10.1038/srep28974, publisher: Nature Publishing Group, 2016.

Liu, D., Zhang, C., Ogaya, R., Acil, N., Pugh, T. A. M., Domene, X., Zhang, X., Fang, Y., Yang, X., Essl, F., Dullinger, S., and Peñuelas, J.: World-wide impacts of climate change and nitrogen deposition on vegetation structure, composition, and functioning of shrublands, New Phytologist, 247, 1117–1128, https://doi.org/10.1111/nph.70235, _eprint: https://nph.onlinelibrary.wiley.com/doi/pdf/10.1111/nph.70235, 2025.

Ma, H., Mo, L., Crowther, T. W., Maynard, D. S., van den Hoogen, J., Stocker, B. D., Terrer, C., and Zohner, C. M.: The global distribution and environmental drivers of aboveground versus belowground plant biomass, Nature Ecology & Evolution, 5, 1110–1122, https://doi.org/10.1038/s41559-021-01485-1, publisher: Nature Publishing Group, 2021.

Ma, S., He, F., Tian, D., Zou, D., Yan, Z., Yang, Y., Zhou, T., Huang, K., Shen, H., and Fang, J.: Variations and determinants of carbon content in plants: a global synthesis, Biogeosciences, 15, 693–702, https://doi.org/10.5194/bg-15-693-2018, 2018.

Martin, A. C., Jeffers, E. S., Petrokofsky, G., Myers-Smith, I., and Macias-Fauria, M.: Shrub growth and expansion in the Arctic tundra: an assessment of controlling factors using an evidence-based approach, Environmental Research Letters, 12, 085 007, https://doi.org/10.1088/1748-9326/aa7989, publisher: IOP Publishing, 2017.

Martin, A. C., Macias-Fauria, M., Bonsall, M. B., Forbes, B. C., Zetterberg, P., and Jeffers, E. S.: Common mechanisms explain nitrogen-dependent growth of Arctic shrubs over three decades despite heterogeneous trends and declines in soil nitrogen availability, New Phytologist, 233, 670–686, https://doi.org/10.1111/nph.17529, _eprint: https://nph.onlinelibrary.wiley.com/doi/pdf/10.1111/nph.17529, 2022.

McCarthy, H. R., Oren, R., Johnsen, K. H., Gallet-Budynek, A., Pritchard, S. G., Cook, C. W., LaDeau, S. L., Jackson, R. B., and Finzi, A. C.: Re-assessment of plant carbon dynamics at the Duke free-air CO2 enrichment site: interactions of atmospheric [CO2] with nitrogen and water availability over stand development, New Phytologist, 185, 514–528, https://doi.org/https://doi.org/10.1111/j.1469-8137.2009.03078.x, 2010.

Mekonnen, Z. A., Riley, W. J., and Grant, R. F.: Accelerated Nutrient Cycling and Increased Light Competition Will Lead to 21st Century Shrub Expansion in North American Arctic Tundra, Journal of Geophysical Research: Biogeosciences, 123, 1683–1701, https://doi.org/10.1029/2017JG004319, _eprint: https://onlinelibrary.wiley.com/doi/pdf/10.1029/2017JG004319, 2018.

Mekonnen, Z. A., Riley, W. J., Berner, L. T., Bouskill, N. J., Torn, M. S., Iwahana, G., Breen, A. L., Myers-Smith, I. H., Criado, M. G., Liu, Y., Euskirchen, E. S., Goetz, S. J., Mack, M. C., and Grant, R. F.: Arctic tundra shrubification: a review of mechanisms and impacts on ecosystem carbon balance, Environmental Research Letters, 16, 053 001, https://doi.org/10.1088/1748-9326/abf28b, publisher: IOP Publishing, 2021.

https://doi.org/10.5194/egusphere-2026-1514
Preprint. Discussion started: 24 March 2026

Meyer, G., Humphreys, E. R., Melton, J. R., Cannon, A. J., and Lafleur, P. M.: Simulating shrubs and their energy and carbon dioxide fluxes in Canada's Low Arctic with the Canadian Land Surface Scheme Including Biogeochemical Cycles (CLASSIC), Biogeosciences, 18, 3263–3283, https://doi.org/10.5194/bg-18-3263-2021, 2021.

Meyerholt, J., Zaehle, S., and Smith, M. J.: Variability of projected terrestrial biosphere responses to elevated levels of atmospheric CO2 due to uncertainty in biological nitrogen fixation, Biogeosciences, 13, 1491–1518, https://doi.org/10.5194/bg-13-1491-2016, 2016.

Miller, P. A. and Smith, B.: Modelling Tundra Vegetation Response to Recent Arctic Warming, AMBIO, 41, 281–291, https://doi.org/10.1007/s13280-012-0306-1, 2012.

Moore, E. R., Pouyat, R. V., and Trammell, T. L. E.: Soil nitrogen cycling in forests invaded by the shrub Rosa multiflora: importance of soil moisture and invasion density, Biogeochemistry, 167, 301–319, https://doi.org/10.1007/s10533-024-01133-3, 2024.

Norby, R. J., Warren, J. M., Iversen, C. M., Medlyn, B. E., and McMurtrie, R. E.: CO₂ enhancement of forest productivity constrained by limited nitrogen availability, Proceedings of the National Academy of Sciences, 107, 19 368–19 373, https://doi.org/10.1073/pnas.1006463107, 2010.

Orndahl, K. M., Berner, L. T., Macander, M. J., Arndal, M. F., Alexander, H. D., Humphreys, E. R., Loranty, M. M., Ludwig, S. M., Nyman, J., Juutinen, S., Aurela, M., Mikola, J., Mack, M. C., Rose, M., Vankoughnett, M. R., Iversen, C. M., Kumar, J., Salmon, V. G., Yang, D., Grogan, P., Danby, R. K., Scott, N. A., Olofsson, J., Siewert, M. B., Deschamps, L., Maire, V., Lévesque, E., Gauthier, G., Boudreau, S., Gaspard, A., Bret-Harte, M. S., Raynolds, M. K., Walker, D. A., Michelsen, A., Kumpula, T., Villoslada, M., Ylänne, H., Luoto, M., Virtanen, T., Greaves, H. E., Forbes, B. C., Heim, R. J., Hölzel, N., Epstein, H., Bunn, A. G., Holmes, R. M., Natali, S. M., Virkkala, A.-M., and Goetz, S. J.: Next generation Arctic vegetation maps: Aboveground plant biomass and woody dominance mapped at 30 m resolution across the tundra biome, Remote Sensing of Environment, 323, 114 717, https://doi.org/10.1016/j.rse.2025.114717, 2025.

Palmtag, J., Obu, J., Kuhry, P., Siewert, M., Weiss, N., and Hugelius, G.: A high spatial resolution soil carbon and nitrogen dataset for the northern permafrost region., https://doi.org/https://doi.org/10.17043/palmtag-2022-spatial-1, 2022.

Parker, T. C., Thurston, A. M., Raundrup, K., Subke, J.-A., Wookey, P. A., and Hartley, I. P.: Shrub expansion in the Arctic may induce large-scale carbon losses due to changes in plant-soil interactions, Plant and Soil, 463, 643–651, https://doi.org/10.1007/s11104-021-04919-8, 2021.

Pirk, N., Aalstad, K., Mannerfelt, E. S., Clayer, F., de Wit, H., Christiansen, C. T., Althuizen, I., Lee, H., and Westermann, S.: Disaggregating the Carbon Exchange of Degrading Permafrost Peatlands Using Bayesian Deep Learning, Geophysical Research Letters, 51, e2024GL109 283, https://doi.org/https://doi.org/10.1029/2024GL109283, 2024.

Poley, L. G., Laskin, D. N., and McDermid, G. J.: Quantifying Aboveground Biomass of Shrubs Using Spectral and Structural Metrics Derived from UAS Imagery, Remote Sensing, 12, 2199, https://doi.org/10.3390/rs12142199, number: 14 Publisher: Multidisciplinary Digital Publishing Institute, 2020.

Poulter, B., MacBean, N., Hartley, A., Khlystova, I., Arino, O., Betts, R., Bontemps, S., Boettcher, M., Brockmann, C., Defourny, P., Hagemann, S., Herold, M., Kirches, G., Lamarche, C., Lederer, D., Ottlé, C., Peters, M., and Peylin, P.: Plant functional type classification for earth system models: results from the European Space Agency's Land Cover Climate Change Initiative, Geoscientific Model Development, 8, 2315–2328, https://doi.org/10.5194/gmd-8-2315-2015, 2015.

Prager, C. M., Naeem, S., Boelman, N. T., Eitel, J. U. H., Greaves, H. E., Heskel, M. A., Magney, T. S., Menge, D. N., Vierling, L. A., and Griffin, K. L.: A gradient of nutrient enrichment reveals nonlinear impacts of fertilization on Arctic plant diversity and ecosystem function, Ecology and Evolution, 7, 2449–2460, https://doi.org/10.1002/ece3.2863, 2017.

https://doi.org/10.5194/egusphere-2026-1514
Preprint. Discussion started: 24 March 2026

Running, S. and Zhao, M.: MODIS/Terra Gross Primary Productivity Gap-Filled 8-Day L4 Global 500m SIN Grid V061., https://doi.org/10.5067/MODIS/MOD17A2HGF.061, 2021.

Running, S., Mu, Q., and Zhao, M.: MOD17A2H MODIS/Terra Gross Primary Productivity 8-Day L4 Global 500m SIN Grid V006., https://doi.org/10.5067/MODIS/MOD17A2H.006, 2015.

Schore, A. I. G., Fraterrigo, J. M., Salmon, V. G., Yang, D., and Lara, M. J.: Nitrogen fixing shrubs advance the pace of tall-shrub expansion in low-Arctic tundra, Communications Earth & Environment, 4, 421, https://doi.org/10.1038/s43247-023-01098-5, publisher: Nature Publishing Group, 2023.

Schuur, E. A., Abbott, B. W., Commane, R., Ernakovich, J., Euskirchen, E., Hugelius, G., Grosse, G., Jones, M., Koven, C., Leshyk, V., Lawrence, D., Loranty, M. M., Mauritz, M., Olefeldt, D., Natali, S., Rodenhizer, H., Salmon, V., Schädel, C., Strauss, J., Treat, C., and Turetsky, M.: Permafrost and Climate Change: Carbon Cycle Feedbacks From the Warming Arctic, Annual Review of Environment and Resources, 47, 343–371, https://doi.org/10.1146/annurev-environ-012220-011847, 2022.

Schuur, E. a. G., McGuire, A. D., Schädel, C., Grosse, G., Harden, J. W., Hayes, D. J., Hugelius, G., Koven, C. D., Kuhry, P., Lawrence, D. M., Natali, S. M., Olefeldt, D., Romanovsky, V. E., Schaefer, K., Turetsky, M. R., Treat, C. C., and Vonk, J. E.: Climate change and the permafrost carbon feedback, Nature, 520, 171–179, https://doi.org/10.1038/nature14338, publisher: Nature Publishing Group, 2015.

Shaver, G. R., Bret-Harte, M. S., Jones, M. H., Johnstone, J., Gough, L., Laundre, J., and Chapin III, F. S.: SPECIES COMPOSITION INTERACTS WITH FERTILIZER TO CONTROL LONG-TERM CHANGE IN TUNDRA PRODUCTIVITY, Ecology, 82, 3163–3181, https://doi.org/https://doi.org/10.1890/0012-9658(2001)082[3163:SCIWFT]2.0.CO;2, 2001.

Street, L. E. and Caldararu, S.: Why are Arctic shrubs becoming more nitrogen limited?, New Phytologist, 233, 585–587, https://doi.org/https://doi.org/10.1111/nph.17841, 2022.

Sulman, B. N., Salmon, V. G., Iversen, C. M., Breen, A. L., Yuan, F., and Thornton, P. E.: Integrating Arctic Plant Functional Types in a Land Surface Model Using Above- and Belowground Field Observations, Journal of Advances in Modeling Earth Systems, 13, e2020MS002 396, https://doi.org/10.1029/2020MS002396, _eprint: https://onlinelibrary.wiley.com/doi/pdf/10.1029/2020MS002396, 2021.

Tang, X., Li, H., Huang, N., Li, X., Xu, X., Ding, Z., and Xie, J.: A comprehensive assessment of MODIS-derived GPP for forest ecosystems using the site-level FLUXNET database, Environmental Earth Sciences, 74, 5907–5918, 2015.

Thum, T., Nabel, J. E. M. S., Tsuruta, A., Aalto, T., Dlugokencky, E. J., Liski, J., Luijkx, I. T., Markkanen, T., Pongratz, J., Yoshida, Y., and Zaehle, S.: Evaluating two soil carbon models within the global land surface model JSBACH using surface and spaceborne observations of atmospheric CO2, Biogeosciences, 17, 5721–5743, https://doi.org/10.5194/bg-17-5721-2020, publisher: Copernicus GmbH, 2020.

Treml, V., Hejda, T., and Kašpar, J.: Differences in growth between shrubs and trees: How does the stature of woody plants influence their ability to thrive in cold regions?, Agricultural and Forest Meteorology, 271, 54–63, https://doi.org/10.1016/j.agrformet.2019.02.036, 2019.

Virkkala, A.-M., Rogers, B., Watts, J., Arndt, K., Potter, S., Wargowsky, I., Schuur, E., See, C., Mauritz, M., Boike, J., Bret-Harte, M., Burke, E., Burrell, A., Chae, N., Chatterjee, A., Chevallier, F., Christensen, T. R., Commane, R., Dolman, H. A., and Natali, S.: Wildfires offset the increasing but spatially heterogeneous Arctic–boreal CO2 uptake, Nature Climate Change, 15, 188–195, https://doi.org/10.1038/s41558-024-02234-5, 2025a.

Virkkala, A.-M., Wargowsky, I., Vogt, J., Kuhn, M. A., Madaan, S., O'Keefe, R., Windholz, T., Arndt, K. A., Rogers, B. M., Watts, J. D., Kent, K., Göckede, M., Olefeldt, D., Rocher-Ros, G., Schuur, E. A. G., Bastviken, D., Aalstad, K., Aho, K., Ala-Könni, J., Alcock, H., Althuizen, I., Arp, C. D., Asanuma, J., Attermeyer, K., Aurela, M., Balathandayuthabani, S., Barr, A., Barret, M., Batkhishig, O., Biasi, C., Björkman, M. P., Black, A., Blanc-Betes, E., Bodmer, P., Boike, J., Bolek, A., Bouchard, F., Bussmann, I., Cabrol, L., Canfora, E., Carey,

https://doi.org/10.5194/egusphere-2026-1514
Preprint. Discussion started: 24 March 2026

S., Castro-Morales, K., Chae, N., Christen, A., Christensen, T. R., Christiansen, C. T., Chu, H., Clark, G., Clayer, F., Crill, P., Cunada, C., Davidson, S. J., Dean, J. F., Dengel, S., Detto, M., Dieleman, C., Domine, F., Dyukarev, E., Edgar, C., Elberling, B., Emmerton, C. A., Euskirchen, E., Falvo, G., Friborg, T., Garneau, M., Giamberini, M., Glagolev, M. V., Gonzalez-Meler, M. A., Granath, G., Guðmundsson, J., Happonen, K., Harazono, Y., Harris, L., Hashemi, J., Hasson, N., Heerah, J., Heffernan, L., Helbig, M., Helgason, W., Heliasz, M., Henry, G., Hensgens, G., Hiyama, T., Hock, M., Holl, D., Holmes, B., Holst, J., Holst, T., Hould-Gosselin, G., Humphreys, E., Hung, J., Huotari, J., Ikawa, H., Ilyasov, D. V., Ishikawa, M., Iwahana, G., Iwata, H., Jackowicz-Korczynski, M. A., Jansen, J., Järveoja, J., Jassey, V. E. J., Jensen, R., Jentzsch, K., Jespersen, R. G., Johannesson, C.-F., Jones, C. P., Jonsson, A., Jung, J. Y., Juutinen, S., Kane, E., Karlsson, J., Karsanaev, S., Kasak, K., Kelly, J., Kempton, K., Klaus, M., Kling, G. W., Kljun, N., Knutson, J., Kobayashi, H., Kochendorfer, J., Kohonen, K.-M., Kolari, P., Korkiakoski, M., Korrensalo, A., Kortelainen, P., Koster, E., Koster, K., Kotani, A., Krishnan, P., Kurbatova, J., Kutzbach, L., Kwon, M. J., Kyzivat, E. D., Lagroix, J., Langhorst, T., Lapshina, E., Larmola, T., Larsen, K. S., Laurion, I., Ledman, J., Lee, H., Leffler, A. J., Lesack, L., Lindroth, A., Lipson, D., Lohila, A., López-Blanco, E., St. Louis, V. L., Lundin, E., Luoto, M., Machimura, T., Magnani, M., Malhotra, A., Maljanen, M., Mammarella, I., Männistö, E., Marchesini, L. B., Marsh, P., Martkainen, P. J., Marushchak, M. E., Mastepanov, M., Mavrovic, A., Maximov, T., Minions, C., Montemayor, M., Morishita, T., Murphy, P., Nadeau, D. F., Nicholls, E., Nilsson, M. B., Niyazova, A., Nordén, J., Noumonvi, K. D., Nykanen, H., Oechel, W., Ojala, A., Okadera, T., Pal, S., Panov, A. V., Papakyriakou, T., Papale, D., Park, S.-J., Parmentier, F.-J. W., Pastorello, G., Peacock, M., Peichl, M., Petrov, R., St. Pierre, K., Pirk, N., Plein, J., Preskienis, V., Prokushkin, A., Pumpanen, J., Rains, H. A., Rakos, N., Räsänen, A., Rautakoski, H., Rinnan, R., Rinne, J., Rocha, A., Roulet, N., Roy, A., Rutgersson, A., Sabrekov, A. F., Sachs, T., Sahlée, E., Salazar, A., Sawakuchi, H. O., Schulze, C., Seco, R., Sepulveda-Jauregui, A., Serikova, S., Serrone, A., Silvennoinen, H. M., Sjogersten, S., Skeeter, J., Snöälv, J., Sobek, S., Sonnentag, O., Stanley, E. H., Strack, M., Strom, L., Sullivan, P., Sullivan, R., Sytiuk, A., Tagesson, T., Taillardat, P., Talbot, J., Tank, S. E., Tenuta, M., Terenteva, I., Thalasso, F., Thiboult, A., Thorgeirsson, H., Garcia Tigreros, F., Torn, M., Townsend-Small, A., Treat, C., Tremblay, A., Trotta, C., Tuittila, E.-S., Turetsky, M., Ueyama, M., Umair, M., Vähä, A., van Delden, L., van Hardenbroek, M., Varlagin, A., Varner, R. K., Veretennikova, E., Vesala, T., Virtanen, T., Voigt, C., Vonk, J. E., Wagner, R., Walter Anthony, K., Wang, Q., Watanabe, M., Webb, H., Welker, J. M., Westergaard-Nielsen, A., Westermann, S., White, J. R., Wille, C., Williamson, S. N., Zolkos, S., Zona, D., and Natali, S. M.: ABCFlux v2: Arctic–boreal CO_2 and CH_4 monthly flux observations and ancillary information across terrestrial and freshwater ecosystems, Earth System Science Data Discussions, 2025, 1–86, https://doi.org/10.5194/essd-2025-585, 2025b.

Vowles, T. and Bjoerk, R. G.: Implications of evergreen shrub expansion in the Arctic, Journal of Ecology, 107, 650–655, https://doi.org/10.1111/1365-2745.13081, _eprint: https://onlinelibrary.wiley.com/doi/pdf/10.1111/1365-2745.13081, 2019.

Wang, L., Zhu, H., Lin, A., Zou, L., Qin, W., and Du, Q.: Evaluation of the latest MODIS GPP products across multiple biomes using global eddy covariance flux data, Remote Sensing, 9, 418, 2017.

Wang, P., Heijmans, M. M., Mommer, L., van Ruijven, J., Maximov, T. C., and Berendse, F.: Belowground plant biomass allocation in tundra ecosystems and its relationship with temperature, Environmental Research Letters, 11, 055 003, 2016.

Wei, T., Li, J., Rong, X., Dong, W., Wu, B., and Ding, M.: Arctic climate changes based on historical simulations (1900–2013) with the CAMS-CSM, Journal of Meteorological Research, 32, 881–895, https://doi.org/https://doi.org/10.1007/s13351-018-7188-5, 2018.

Yu, T. and Zhuang, Q.: Modeling biological nitrogen fixation in global natural terrestrial ecosystems, Biogeosciences, 17, 3643–3657, https://doi.org/10.5194/bg-17-3643-2020, publisher: Copernicus GmbH, 2020.

Zaehle, S. and Friend, A. D.: Carbon and nitrogen cycle dynamics in the OCN land surface model: 1. Model description, site-scale evaluation, and sensitivity to parameter estimates, Global Biogeochemical Cycles, 24, https://doi.org/10.1029/2009GB003521, _eprint: https://onlinelibrary.wiley.com/doi/pdf/10.1029/2009GB003521, 2010.

https://doi.org/10.5194/egusphere-2026-1514
Preprint. Discussion started: 24 March 2026

Zhang, W., Miller, P. A., Smith, B., Wania, R., Koenigk, T., and Döscher, R.: Tundra shrubification and tree-line advance amplify arctic climate warming: results from an individual-based dynamic vegetation model, Environmental Research Letters, 8, 034 023, https://doi.org/10.1088/1748-9326/8/3/034023, publisher: IOP Publishing, 2013.

Zhao, Y., Liu, X., Wang, Y., Zheng, Z., Zheng, S., Zhao, D., and Bai, Y.: UAV-based individual shrub aboveground biomass estimation calibrated against terrestrial LiDAR in a shrub-encroached grassland, International Journal of Applied Earth Observation and Geoinformation, 101, 102 358, https://doi.org/10.1016/j.jag.2021.102358, 2021.

Zhao, Y., Wang, H., Ma, Y., Li, Z., Mi, W., and Cao, Z.: Spatial estimation of soil carbon and nitrogen in a grassland shrubland transition, Ecological Indicators, 153, 110 384, https://doi.org/10.1016/j.ecolind.2023.110384, 2023.

Zhou, Y., Sha, M., Jin, H., Wang, L., Zhang, J., Xu, Z., Tan, B., Chen, L., Wang, L., Liu, S., Xiao, J., You, C., Huang, Y., Chen, Y., and Liu, Y.: The expansion of evergreen and deciduous shrubs changed the chemical characteristics and biological community of alpine meadows soil, European Journal of Soil Biology, 117, 103 505, https://doi.org/https://doi.org/10.1016/j.ejsobi.2023.103505, 2023.

Zhu, X., Pei, Y., Zheng, Z., Dong, J., Zhang, Y., Wang, J., Chen, L., Doughty, R. B., Zhang, G., and Xiao, X.: Underestimates of grassland gross primary production in MODIS standard products, Remote Sensing, 10, 1771, 2018.

https://doi.org/10.5194/egusphere-2026-1514
Preprint. Discussion started: 24 March 2026

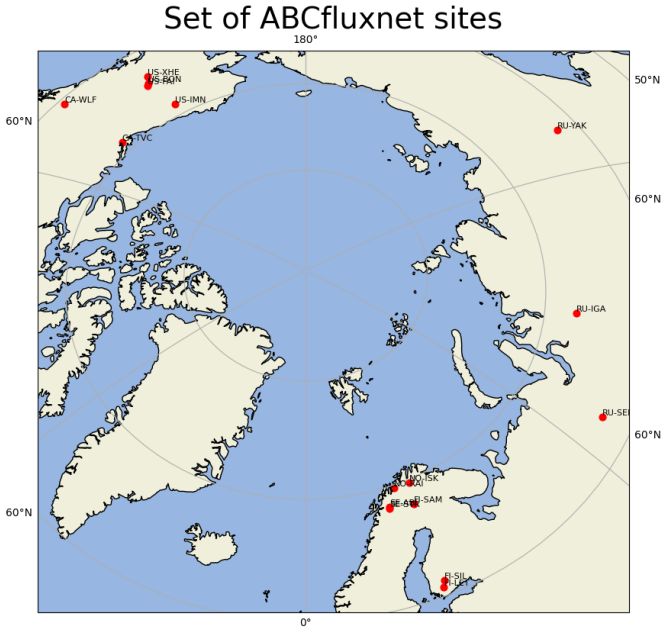

Figure A1. Map of the 16 chosen stations.

Table A1. List of the study sites with coordinates and soil forcing specifying the clay, silt and sand soil proportion, the bulk density (bd) of organic matter [kg m-3], the available water content (awc), the ph value, usda taxonomy class, nwrb taxonomy class and the initial phosphoros pools (labile, slow, occulded and primary) in the soil [g m-2]. The initial soil depth for phosphorus is 0.5 m.

Site-ID	lon	lat	PFT	clay	silt	sand	awc	bd	ph	taxusda	taxnwrb	soilP,labile	soilP,slow	soilP,occluded	soilP,primary
WLF (Wolf Creek, Canada)	-135.25	60.75	BD	0.13	0.26	0.61	540	1094	6.16	89	27	32.46	50.94	169.07	84.31
TVC (Trail valley Creek, Canada)	-133.75	68.75	NE	0.30	0.41	0.29	400	1046	5.19	6	40	28.42	35.16	109.51	54.85
LET (Lettosuo, Finland)	23.75	60.75	BD	0.19	0.30	0.51	406.14	1186	5.39	36	27	30.09	50.58	120.21	39.90
SIL (Siikaneva, Finland)	24.25	61.25	BD	0.14	0.33	0.53	441	1194	5.33	18	27	26.75	44.96	106.9	35.46
SAM (Sammaltunturi fell, Finland)	24.15	67.97	NE	0.07	0.34	0.59	491.9	1148	5.19	89	27	28	35.16	110	54.85
ISK (Iskoras, Norway)	25.25	69.75	NE	0.06	0.35	0.59	548.9	1152	5.3	89	27	21.73	36.53	86.82	28.81
RAI (Raisduoddar, Norway)	21.25	69.75	NE	0.06	0.32	0.62	424	1159	5.51	33	98	21.73	36.53	86.82	28.81
IGA (Igarka, Russia)	86.25	67.25	BD	0.19	0.39	0.42	599	840.1	5.5	6	39	21.54	33.79	112.2	55.94
SEI (Seida, Russia)	62.75	67.25	BD	0.14	0.41	0.45	554.9	865.6	5.31	5	27	28.42	35.16	109.51	54.85
YAK (Yakutsk, Russia)	129.75	62.25	NE	0.18	0.46	0.36	400.0	1166	6.64	6	39	38.59	60.55	201.0	100.2
STR (Stordalen, Sweden)	18.75	68.25	NE	0.07	0.35	0.58	354.1	1148	5.69	89	39	21.54	33.79	112.2	55.94
ABI (Abisko, Sweden)	18.82	68.35	NE	0.07	0.37	0.56	492	1183	5.8	89	27	21.54	33.79	112.2	55.94
FAI (Fairbanks, US)	-147.75	64.88	BD	0.09	0.64	0.27	487.7	1079	6.24	69	25	39.7715	23.08	73.31	54.85
IMN (Imnavait Creek, US)	-149.3	68.61	BD	0.17	0.38	0.45	473	703	5.76	6	27	28.42	35.16	109.5	54.85
BON (Bonanza, US)	-148.25	64.75	NE	0.06	0.63	0.31	475	1097	6.11	77	27	39.77	23.08	73.31	54.85
XHE (NEON healy, US)	-149.21	63.88	NE	0.11	0.44	0.5	506.9	1056	5.37	90	27	21.54	33.79	112.17	55.94

https://doi.org/10.5194/egusphere-2026-1514
Preprint. Discussion started: 24 March 2026

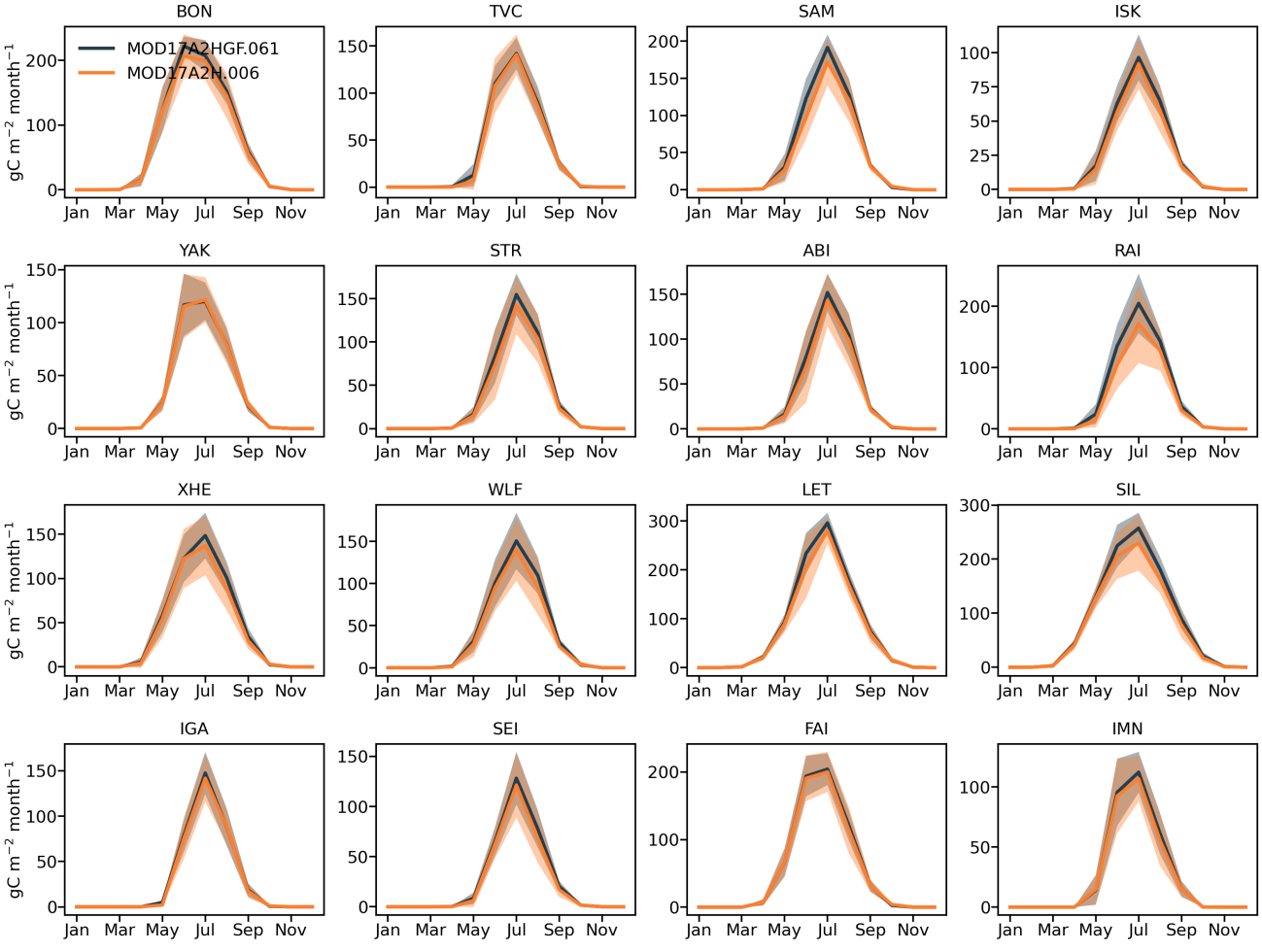

Figure A2. Multi-year (2000-2010) mean seasonal cycle of the standard derivation of GPP derived from two MODIS satellite products (MOD17A2HGF and MOD17A2H).

https://doi.org/10.5194/egusphere-2026-1514
Preprint. Discussion started: 24 March 2026

Table A2. List of the study sites reporting the site reference, dominant vegetation, available data points, used flux method and time period.

Site name	Dominant vegetation	Total number of data points	Flux method	Time
Abisko	Mosses and dwarf evergreen shrubs (e.g. Cassope tetragona, Empetrum hermaphroditum)	47	Automated and manual chamber	1999-2012
Bonanza	evergreen shrubs	162	EC, manual chamber	1990-2020
Igarka	deciduous shrubs	109	EC, manual chamber	2007-2020
Imnavait	deciduous and evergreen shrubs (e.g. Andromeda polifolia, Betula nana)	530	EC, manual chamber	2007-2020
Iskoras	evergreen dwarf shrubs (e.g. Empetrum nigrum, Rhododendron tomentosum)	174	EC, manual chamber	2019-2020
Lettosuo	Evergreen Needleleaf Forests and understory	320	EC, automated chamber	2009-2020
Neon healy	NaN	47	EC	2018-2020
Raisduoddar	deciduous and evergreen shrubs, sedges	9	manual chamber	2014
Sammaltunturi	juniper bushes and low shrubs (e.g. Betula nana, Empetrum hermaphroditum)	12	EC	2012
Seida	deciduous and evergreen shrubs	81	manual chamber, EC	2008-2009
Siikaneva	Scots pine, deciduous and evergreen shrubs (vaccinium, andromeda polifolia)	1245	manual and automated chamber, EC	2007-2020
Stordalen	willow mixed with sedges, lichens	450	manual and automated chamber, EC	1996-2020
Trail Valley Creek	dwarf evergreen shrubs, sedges	372	manual and automated chamber, EC	2013-2020
Wolf Creek	deciduous shrub (e.g. willow), white spruce	297	EC	2017-2020

Table A3. R^2 values between different model versions and observation data (ABCfluxnet data and the mean of the MODIS products) for the available time span of the ABCfluxnet data. If available we use only the EC measurements from the ABCflux data. NaN mark data with too small data size.

sites	CN model vs. ABC	C-only model vs. ABC	CN model vs mean MOD	C-only model vs mean MOD
BON (Bonanza, US)	0.89	0.95	0.92	0.97
TVC (Trail valley Creek, Canada)	0.65	0.91	0.78	0.97
SAM (Sammaltunturi fell, Finland)	NaN	NaN	0.88	0.71
ISK (Iskoras, Norway)	0	0.87	0.86	0
YAK (Yakutsk, Russia)	0.89	0.87	0.54	0.57
STR (Stordalen, Sweden)	0.46	0.93	0.50	0.86
ABI (Abisko, Sweden)	0	0.38	0.53	0.87
RAI (Raisduoddar, Norway)	NaN	NaN	0.51	0.94
XHE (NEON healy, US)	0.88	0	0.84	0.64
WLF (Wolf Creek, Canada)	0.29	0.71	0.53	0.64
LET (Lettosuo, Finland)	0.41	0.88	0.53	0.86
SIL (Siikaneva1, Finland)	0.40	0	0.61	0.92
IGA (Igarka, Russia)	0.42	0.45	0.43	0.44
SEI (Seida, Russia)	0.17	0.70	0.47	0.2
FAI (Fairbanks, US)	NaN	NaN	0.56	0.86
IMN (Imnavait Creek, US)	0.50	0	0.37	0.20
Mean	**0.48**	**0.59**	**0.62**	**0.67**